Published OnlineFirst on October 5, 2011; DOI:10.1158/1078-0432.CCR-11-1712

being planned to validate present observations. It should be noted that specificity, that is, absence of pseudopositive, is most important for new noninvasive diagnostics. The validation study should also be focused on this point as well.

As suggested by a recent review (26), the most problematic aspect of ctDNA analysis is the difficulty in purifying DNA from the blood. As described above, the amount of plasma DNA varies by 2 orders of magnitude. The cause of this variation (i.e., whether it is due to true variation or the low reproducibility of the purification procedure) is unknown. However, it should be noted that unsuccessful mutation detection was not necessarily frequent in the cases with low DNA recovery and that unsuccessful mutation detection was still found among those with abundant DNA recovery. Some cases of low DNA recovery contained the minimum number of *EGFR* copies for detection. In such cases, whole-genome amplification is beneficial for sound PCR and may enhance the detection rate, as seen in a previous study (19).

This study focused on advanced lung cancer (mainly stage IV lung cancer). If ctDNA analysis is effective for early lung cancer, then it may be applicable to early cancer detection. Because ctDNA is also easily detected in the early stages of colorectal cancer (27), it is worthwhile to test ctDNA analysis for early lung cancer.

BEAMing uses the template preparation step of massively parallel sequencers (so-called next-generation sequencers; ref. 28). Therefore, we can predict the outcome when massively parallel sequencers are applied to this problem. The recent development of a new sequencer (29) has addressed the shortcomings of currently available sequencers (i.e., a long runtime for a single assay and high operating costs), and would be suitable for diagnostic purposes. The cost of sequencing is still rapidly decreasing, and will be eventually negligible in the total cost of the assay. In contrast to BEAMing, which analyzes only a single base and requires information about mutations in primary tumors, the massively parallel sequencers obtain information from more than a hundred bases and could replace BEAMing. A recent study pointed out the need for repeated sequencing to overcome the high error rates of the sequencers that are currently used to detect rare mutations (30). However, in the case of *EGFR* mutations, because the mutation sites are already known, rare mutations may be detected with a statistical method without the repeated sequencing. Our study forecasts the outcome of ctDNA analysis using massively parallel sequencers, suggesting that ctDNA analysis could determine the *EGFR* mutation status of more than 70% of advanced lung cancer cases. In addition, there might be cases in which *EGFR* mutations could be detected only with ctDNA analysis, not with a conventional biopsy. Given the noninvasive nature of the ctDNA analysis, it is a worthwhile field for future investigation.

Disclosure of Potential Conflicts of Interest

No potential conflicts of interest were disclosed.

Grant Support

This work was partly supported by KAKENHI 20890299 and 23790636.

The costs of publication of this article were defrayed in part by the payment of page charges. This article must therefore be hereby marked *advertisement* in accordance with 18 U.S.C. Section 1734 solely to indicate this fact.

Received July 4, 2011; revised September 20, 2011; accepted September 23, 2011; published OnlineFirst October 5, 2011.

References

1. Lynch TJ, Bell DW, Sordella R, Gurubhagavatula S, Okimoto RA, Brannigan BW, et al. Activating mutations in the epidermal growth factor receptor underlying responsiveness of non-small-cell lung cancer to gefitinib. N Engl J Med 2004;350:2129–39.
2. Paez JG, Janne PA, Lee JC, Tracy S, Greulich H, Gabriel S, et al. EGFR mutations in lung cancer: correlation with clinical response to gefitinib therapy. Science 2004;304:1497–500.
3. Rosell R, Moran T, Queralt C, Porta R, Cardenal F, Camps C, et al. Screening for epidermal growth factor receptor mutations in lung cancer. N Engl J Med 2009;361:958–67.
4. Kobayashi S, Boggon TJ, Dayaram T, Janne PA, Kocher O, Meyerson M, et al. EGFR mutation and resistance of non-small-cell lung cancer to gefitinib. N Engl J Med 2005;352:786–92.
5. Pao W, Miller VA, Politi KA, Riely GJ, Somwar R, Zakowski MF, et al. Acquired resistance of lung adenocarcinomas to gefitinib or erlotinib is associated with a second mutation in the EGFR kinase domain. PLoS Med 2005;2:e73.
6. Oxnard GR, Arcila ME, Sima CS, Riely GJ, Chmielecki J, Kris MG, et al. Acquired resistance to EGFR tyrosine kinase inhibitors in EGFR-mutant lung cancer: distinct natural history of patients with tumors harboring the T790M mutation. Clin Cancer Res 2011;17:1616–22.
7. Kosaka T, Yatabe Y, Endoh H, Yoshida K, Hida T, Tsuboi M, et al. Analysis of epidermal growth factor receptor gene mutation in patients with non-small cell lung cancer and acquired resistance to gefitinib. Clin Cancer Res 2006;12:5764–9.
8. Goebel G, Zitt M, Zitt M, Muller HM. Circulating nucleic acids in plasma or serum (CNAPS) as prognostic and predictive markers in patients with solid neoplasias. Dis Markers 2005;21:105–20.
9. Vlassov VV, Laktionov PP, Rykova EY. Circulating nucleic acids as a potential source for cancer biomarkers. Curr Mol Med 2010;10:142–65.
10. Diehl F, Schmidt K, Choti MA, Romans K, Goodman S, Li M, et al. Circulating mutant DNA to assess tumor dynamics. Nat Med 2008;14:985–90.
11. Shinozaki M, O'Day SJ, Kitago M, Amersi F, Kuo C, Kim J, et al. Utility of circulating B-RAF DNA mutation in serum for monitoring melanoma patients receiving biochemotherapy. Clin Cancer Res 2007;13:2068–74.
12. Dressman D, Yan H, Traverso G, Kinzler KW, Vogelstein B. Transforming single DNA molecules into fluorescent magnetic particles for detection and enumeration of genetic variations. Proc Natl Acad Sci U S A 2003;100:8817–22.
13. Pao W, Ladanyi M. Epidermal growth factor receptor mutation testing in lung cancer: searching for the ideal method. Clin Cancer Res 2007;13:4954–5.
14. Nagai Y, Miyazawa H, Huqun, Tanaka T, Udagawa K, Kato M, et al. Genetic heterogeneity of the epidermal growth factor receptor in non-small cell lung cancer cell lines revealed by a rapid and sensitive detection system, the peptide nucleic acid-locked nucleic acid PCR clamp. Cancer Res 2005;65:7276–82.
15. Rago C, Huso DL, Diehl F, Karim B, Liu G, Papadopoulos N, et al. Serial assessment of human tumor burdens in mice by the analysis of circulating DNA. Cancer Res 2007;67:9364–70.

Published OnlineFirst on October 5, 2011; DOI:10.1158/1078-0432.CCR-11-1712

16. Diehl F, Schmidt K, Durkee KH, Moore KJ, Goodman SN, Shuber AP, et al. Analysis of mutations in DNA isolated from plasma and stool of colorectal cancer patients. Gastroenterology 2008;135:489–98.
17. Li M, Chen WD, Papadopoulos N, Goodman SN, Bjerregaard NC, Laurberg S, et al. Sensitive digital quantification of DNA methylation in clinical samples. Nat Biotechnol 2009;27:858–63.
18. Kimura H, Kasahara K, Kawaishi M, Kunitoh H, Tamura T, Holloway B, et al. Detection of epidermal growth factor receptor mutations in serum as a predictor of the response to gefitinib in patients with non-small-cell lung cancer. Clin Cancer Res 2006;12:3915–21.
19. Kuang Y, Rogers A, Yeap BY, Wang L, Makrigiorgos M, Vetrand K, et al. Noninvasive detection of EGFR T790M in gefitinib or erlotinib resistant non-small cell lung cancer. Clin Cancer Res 2009;15:2630–6.
20. Brevet M, Johnson ML, Azzoli CG, Ladanyi M. Detection of EGFR mutations in plasma DNA from lung cancer patients by mass spectrometry genotyping is predictive of tumor EGFR status and response to EGFR inhibitors. Lung Cancer 2011;73:96–102.
21. Bai H, Mao L, Wang HS, Zhao J, Yang L, An TT, et al. Epidermal growth factor receptor mutations in plasma DNA samples predict tumor response in Chinese patients with stages IIIB to IV non-small-cell lung cancer. J Clin Oncol 2009;27:2653–9.
22. Inukai M, Toyooka S, Ito S, Asano H, Ichihara S, Soh J, et al. Presence of epidermal growth factor receptor gene T790M mutation as a minor clone in non-small cell lung cancer. Cancer Res 2006;66:7854–8.
23. Soh J, Toyooka S, Ichihara S, Suehisa H, Kobayashi N, Ito S, et al. EGFR mutation status in pleural fluid predicts tumor responsiveness and resistance to gefitinib. Lung Cancer 2007;56:445–8.
24. Giaccone G, Wang Y. Strategies for overcoming resistance to EGFR family tyrosine kinase inhibitors. Cancer Treat Rev 2011;37:456–64.
25. Ercan D, Zejnullahu K, Yonesaka K, Xiao Y, Capelletti M, Rogers A, et al. Amplification of EGFR T790M causes resistance to an irreversible EGFR inhibitor. Oncogene 2010;29:2346–56.
26. Schwarzenbach H, Hoon DS, Pantel K. Cell-free nucleic acids as biomarkers in cancer patients. Nat Rev Cancer 2011;11:426–37.
27. Diehl F, Li M, Dressman D, He Y, Shen D, Szabo S, et al. Detection and quantification of mutations in the plasma of patients with colorectal tumors. Proc Natl Acad Sci U S A 2005;102:16368–73.
28. Margulies M, Egholm M, Altman WE, Attiya S, Bader JS, Bemben LA, et al. Genome sequencing in microfabricated high-density picolitre reactors. Nature 2005;437:376–80.
29. Rothberg JM, Hinz W, Rearick TM, Schultz J, Mileski W, Davey M, et al. An integrated semiconductor device enabling non-optical genome sequencing. Nature 2011;475:348–52.
30. Kinde I, Wu J, Papadopoulos N, Kinzler KW, Vogelstein B. Detection and quantification of rare mutations with massively parallel sequencing. Proc Natl Acad Sci U S A 2011;108:9530–5.

Glycobiology vol. 20 no. 12 pp. 1594–1606, 2010
doi: 10.1093/glycob/cwq108
Advance Access publication on July 28, 2010

Novel ganglioside found in adenocarcinoma cells of Lewis-negative patients

Kyoko Shida[2], Hiroaki Korekane[3], Yoshiko Misonou[2], Shingo Noura[4], Masayuki Ohue[4], Hidenori Takahashi[4], Hiroaki Ohigashi[4], Osamu Ishikawa[4], and Yasuhide Miyamoto[1,2]

[2]Department of Immunology, Osaka Medical Center for Cancer and Cardiovascular Diseases, 1-3-2 Nakamichi, Higashinari-ku, Osaka 537-8511, Japan; [3]Department of Disease Glycomics, The Institute of Scientific and Industrial Research, Osaka University, 8-1 Mihogaoka, Ibaraki, Osaka 567-0047, Japan; and [4]Department of Surgery, Osaka Medical Center for Cancer and Cardiovascular Diseases, 1-3-3 Nakamichi, Higashinari-ku, Osaka 537-8511, Japan

Received on April 19, 2010; revised on July 8, 2010; accepted on July 9, 2010

We have precisely analyzed the structures of glycosphingolipids of human cancer cells and normal epithelial cells using several methods, including enzymatic release of carbohydrate moieties, fluorescent labeling, and identification using 2D mapping, enzymatic digestion, and mass spectrometry. These analyses enabled the identification of novel tumor-associated carbohydrate antigens that can be used to elucidate the involvement of carbohydrates in cancer malignancy and could act as candidate tumor markers. In our previous study, we identified a novel glycosphingolipid that accumulates in colon cancer cells, NeuAcα2-6(Fucα1-2)Galβ1-4GlcNAcβ1-3Galβ1-4Glc (α2-6 sialylated type 2H, ST2H). Here, structural analyses of cancer cells and normal epithelial cells from 60 colorectal and five pancreatic cancer patients, including four and two Lewis-negative individuals, respectively, reveal the presence of an additional novel glycosphingolipid, NeuAcα2-6(Fucα1-2)Galβ1-3GlcNAcβ1-3Galβ1-4Glc (α2-6 sialylated type 1H, ST1H). ST2H was found in colorectal and pancreatic cancer cells from about half of the cases. Unlike ST2H, ST1H was found in cancer cells from three out of six Lewis-negative patients (i.e., two cases of colorectal and one case of pancreatic cancer). However, the moiety was not found in normal epithelial cells or cancer cells from 59 Lewis-positive patients. These findings suggest that the accumulation of this carbohydrate antigen occurs predominantly in cancer cells of Lewis-negative patients. When the ST1H epitope is also carried on mucins as well as glycosphingolipids, this epitope is a promising tumor marker candidate, especially for Lewis-negative individuals.

Keywords: colorectal cancer/glycosphingolipid/Lewis type/pancreatic cancer

Introduction

Drastic alterations in glycosphingolipids (GSLs) and glycoproteins have been observed in a variety of human cancers, and many altered carbohydrate determinants, including sialyl Le^x (SLe^x) and sialyl Le^a (SLe^a), are classified as tumor-associated carbohydrate antigens (Hakomori 1989; Hakomori 2002). A subsequent series of studies have indicated the functional significance of tumor-associated carbohydrate antigens in cancer malignancy, such as metastasis and invasion (Fukuda 1996; Hakomori 1996). For example, SLe^a and SLe^x function as ligands for selectins and are thought to be involved in hematogeneous metastasis (Kannagi et al. 2004). Furthermore, tumor-associated carbohydrate determinants have been utilized as useful tumor markers for the diagnosis of cancer (Kannagi et al. 2004). CA19-9, SLe^a epiotope, is one of the most well-known serum tumor markers and is frequently used for clinical diagnosis of a variety of cancers such as pancreatic, colorectal, and stomach cancers. Thus, identification of novel tumor-associated carbohydrate antigens should give important clues concerning the involvement of carbohydrates in cancer malignancy as well as providing potentially useful tumor markers.

We previously identified a novel tumor-associated carbohydrate antigen in the GSLs from human colon cancer, NeuAcα2-6(Fucα1-2)Galβ1-4GlcNAcβ1-3Galβ1-4Glc (α2-6 sialylated type 2H, abbreviated as ST2H), which is an isomer of SLe^a and SLe^x (Korekane et al. 2007). We have analyzed the structures of GSLs derived from colorectal cancer cells and normal colorectal epithelial cells from 16 patients (Misonou et al. 2009). ST2H was found in colorectal cancer cells from half of the cases. Moreover, ST2H was found in colorectal cancer cells from most of the cases of colorectal cancer cells having hepatic metastasis. ST2H was not found in normal epithelial cells from all the 16 cases. A biosynthetic pathway of ST2H is proposed in Figure 4.

It is well known that the histo-blood group-related carbohydrate antigens, ABH and Lewis, are genetically defined (Nishihara et al. 1994; Kudo et al. 1996; Hakomori 1999). Lewis enzyme (also called FUT3) is the only enzyme responsible for the synthesis of Lewis antigens, such as Le^a, Le^b, and SLe^a in vivo (Kukowska-Latallo et al. 1990) (ref, Figure 4). Lewis-negative individuals, who make up approximately 10% of the population, are homozygotes for the inactive Lewis gene alleles (Mollicone et al. 1994; Nishihara et al. 1994; Elmgren et al. 1997). Such individuals do not possess Lewis enzyme activity and never express Le^a, Le^b, and SLe^a in any tissue (Yazawa et al. 1995; Narimatsu et al. 1996; Nishihara et al. 1999).

In order to discover additional tumor-associated carbohydrate antigens, structural analyses of GSLs of cancer cells

[1]To whom correspondence should be addressed: Tel.: +81-6-6972-1181; Fax: +81-6-6972-7749; E-mail: miyamoto-ya@mc.pref.osaka.jp

Table I. Clinicopathological information on the six Lewis-negative patients with colorectal (cases 1–4) or pancreatic adenocarcinoma (cases 5 and 6)

No	Age	Sex	Tumor localization	Tumor size (mm)	Histological differentiation	Depth of invasion	LN*	LM*	Blood type	CEA (ng/mL)	CA19-9 (U/mL)
1	58	F	Sigmoid	55 × 50	Moderate	SE*	N3	H2	O	27.0	0
2	65	M	Transverse	85 × 50	Moderate	SS*	N0	H1	B	17.7	0
3	53	M	Sigmoid	44 × 33	Moderate	SS	N1	H1	A	3.6	0
4	68	M	Rectum	60 × 50	Well	SS	N1	H0	O	1.0	0
5	85	F	Body	22	Well	T3	N0	H0	A	N.D.*	0
6	66	F	Head	24	Well	T3	N1	H0	A	1.4	0

LN, lymph node metastasis; LM, liver metastasis; SE, serosa exposed; SS, subserosa; N.D., not determined.

have been undertaken. We have analyzed samples from 60 colorectal cancer and five pancreatic cancer patients, including four and two genuine Lewis-negative patients, respectively. We have identified a novel tumor-associated carbohydrate antigen. The antigen accumulates chiefly in cancer cells from Lewis-negative individuals and is a promising candidate tumor marker, especially for Lewis-negative individuals.

Results

Determination of Lewis types

The structural analyses of GSLs of cancer cells and normal epithelial cells from 65 cancer patients (60 cases of colorectal cancer and five cases of pancreatic cancer) were carried out. Among the 65 cases, 56 cases of colorectal cancer patients and three cases of pancreatic cancer patients were determined to be Lewis positive. High levels of Le^a and Le^b structures were observed in GSLs of cancer cells and normal epithelial cells from all the Lewis-positive cases with serum values of CA19-9, a SLe^a determinant, of more than 5 U/mL. The other four cases of colorectal cancer patients (cases 1–4) and two cases of pancreatic cancer patient (cases 5 and 6) were determined to be genuine Lewis negative. The incidence of Lewis-negative individuals (six out of 65) is in good agreement with the anticipated frequency in the population (i.e., 10%). The clinicopathological features of the six patients are described in Table I. Le^a structures were either absent or barely detected in GSLs of cancer cells and normal epithelial cells from these six patients. Moreover, serum CA19-9 values of these patients are 0 U/mL (Table I). Genotyping of the Lewis gene and Lewis enzyme activity were also examined. The full open reading frames of the Lewis gene from all six patients were sequenced. All of the six patients were homozygotes of previously reported null Lewis gene alleles. Cases 1–5 possess two point mutations, T59G and G508A, in both alleles (Nishihara et al. 1994). Case 6 was found to possess two point mutations, T59G and G508A, and another two point mutations, T202C and C314T, in each allele (Elmgren et al. 1997). In addition, as predicted, Lewis activity (α1-4 fucosyltransferase) was not detected to any extent in cancer cells as well as normal colorectal and pancreatic cells of the six cases (data not shown).

Structural analysis of pyridylaminated (PA)-oligosaccharides prepared from colorectal and pancreatic adenocarcinoma cells of Lewis-negative patients having novel tumor-associated carbohydrate antigen

We found a novel GSL in the cancer cells from three out of 65 patients (two colorectal and one pancreatic cancer) who were all Lewis-negative individuals (cases 1, 4, and 6 in Table I). This GSL was not found in normal colorectal and pancreatic epithelial cells from any of the 65 cases. Since the structures of the GSLs of the cancer cells from the three patients were very similar, only the structures of GSLs of rectal cancer cells from case 4 and pancreatic cancer cells from case 6 are shown. Figure 1A shows the acidic and neutral PA-oligosaccharides from rectal cancer cells and normal rectal epithelial cells from case 4. Ten peaks (A1–A10) and 12 peaks (N1–N12) were obtained from acidic and neutral GSLs of rectal cancer cells, respectively (Figure 1A, a and c). Each of the peaks was further purified by reversed-phase high-performance liquid chromatography (HPLC). Peak A8 was separated into three major components, and peaks N6, N7, N9, and N10 were each separated into two major components by reversed-phase HPLC. The peaks were designated A8-1, A8-2, A8-3, N6-1, N6-2, N7-1, N7-2, N9-1, N9-2, N10-1, and N10-2 (Figure 1A, a and c). Ten peaks (A1-A8, A11, A12) and 12 peaks (N1-N10, N12, N13) were obtained from acidic and neutral GSLs of normal rectal epithelial cells, respectively (Figure 1A, b and d). Peak A8 of normal rectal epithelial cells comprised one major component, which corresponds to A8-1 of rectal cancer cells (Figure 1A, b). Peaks N6, N7, N9, and N10 of normal rectal epithelial cells were separated into two major components, similar to rectal cancer cells (Figure 1A, d).

Figure 1B shows the acidic and neutral PA-oligosaccharides from pancreatic cancer cells and normal pancreatic epithelial cells from case 6. Eight peaks (A1–A4, A6–A8, A11) and 11 peaks (N1–N9, N12, N14) were obtained from the acidic and neutral GSLs of pancreatic cancer cells, respectively (Figure 1B, a and c). Six peaks (A1, A3, A4, A7, A13, A14) and 10 peaks (N1-N8, N14, N15) were obtained from the acidic and neutral GSLs of normal pancreatic epithelial cells, respectively (Figure 1B, b and d). Peak A8 of case 6 was separated into two major components by reversed-phase HPLC, corresponding to A8-1 and A8-2 of case 4 (Figure 1B, a). The other peaks from the pancreatic cancer and normal pancreatic cells were shown to comprise a single major component by

reversed-phase HPLC. Peaks N6, N7, and N9 corresponded to N6-1, N7-1, and N9-1 of case 4, respectively (Figure 1B, c and d). A comparison was carried out between the positions on the map and the positions of standard PA-oligosaccharides. With the exception of A8-2, all other peaks matched the standard oligosaccharides (data not shown). The structures of the matched oligosaccharides were also confirmed by mass spectrometry. The predicted structures of the acidic and neutral GSLs of cancer cells and normal epithelial cells from cases 4 and 6 are presented in Tables II and III, respectively.

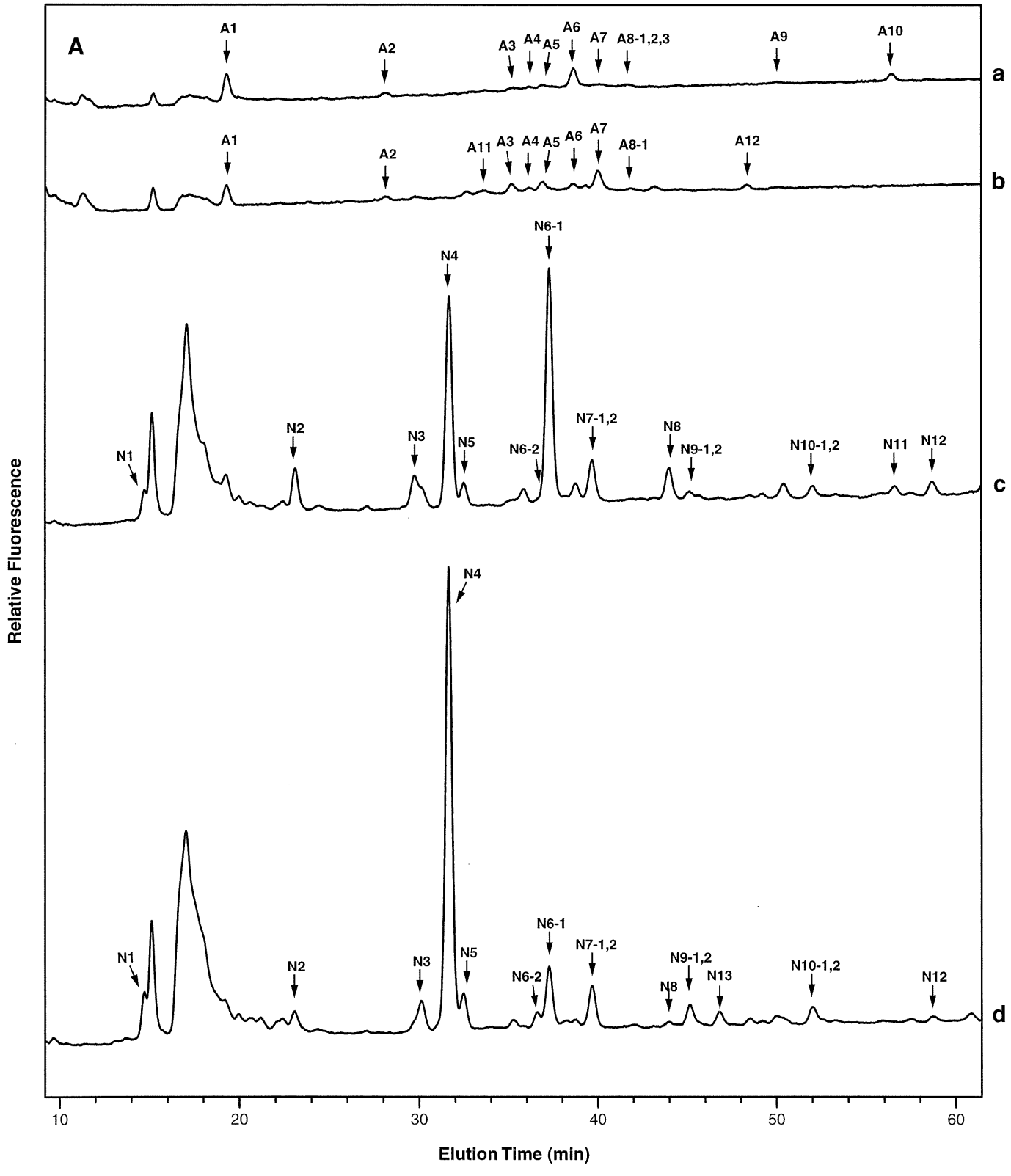

1596

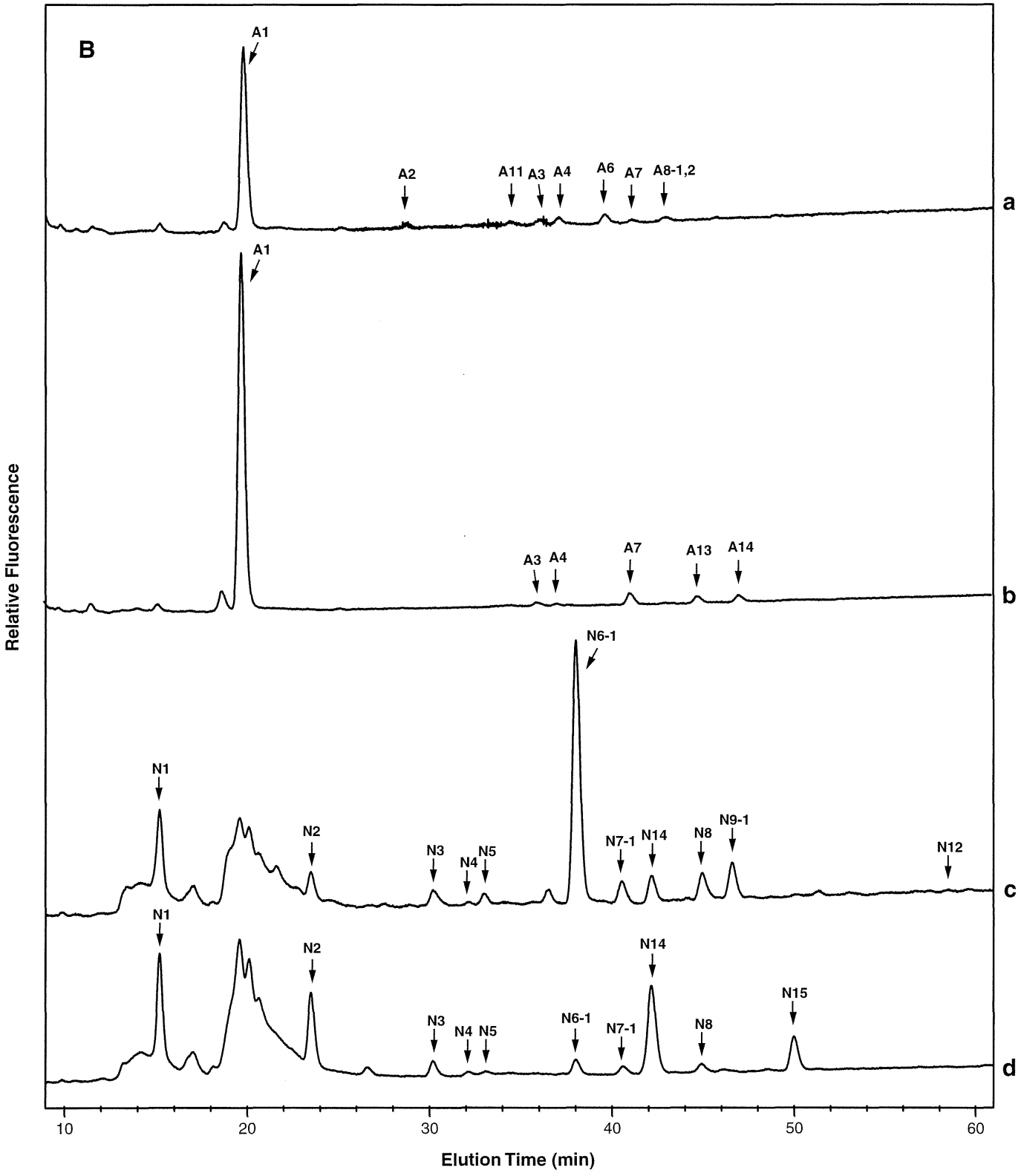

Fig. 1. Size fractionation HPLC of acidic and neutral PA-oligosaccharide mixtures obtained from rectal cancer and normal rectal epithelial cells from case 4 (**A**) and pancreatic cancer and normal pancreatic epithelial cells from case 6 (**B**). **A** and **B**: a, acidic fraction of cancer cells; b, acidic fraction of normal epithelial cells; c, neutral fraction of cancer cells; d, neutral fraction of normal epithelial cells. Identified PA-oligosaccharides in each peak are highlighted with an arrow and numbered with fraction numbers as per Tables II and III. Reverse-phase HPLC separated some of the peaks into two or three components (indicated by the numbers given after the hyphen). Peaks at around 20 min in **A** and **B**, c, and other minor peaks without arrows are artifacts and not PA-oligosaccharides derived from GSLs, as confirmed by mass spectrometry.

The common feature of the profiles of the GSLs from cases 4 and 6 is that Type 1H (N6-1) is greatly increased during carcinogenesis to become the dominant peak (Figure 1A and B, c). This was also observed in the profile of GSLs from case 1. Furthermore, two additional observations regarding the expression of Lewis antigen in Lewis-negative individuals are noteworthy. Firstly, although it is thought that Lewis antigens such as Le^a, Le^b, and SLe^a are not expressed in any tissues of

Table II. Estimated structures of acidic and neutral PA-oligosaccharides from rectal cancer and normal rectal epithelial cells of case 4 (C, cancer cells; N, normal epithelial cells)

Fraction	Structure	Abbreviation	Ratio (%)	
			C	N
acidic				
A1	Neu5Acα2-3Galβ1-4Glc-PA	GM3	3.6	1.7
A2	Neu5Acα2-8Neu5Acα2-3Galβ1-4Glc-PA	GD3	0.3	0.2
A11	Galβ1-3GalNAcβ1-4Galβ1-4Glc-PA 3 | Neu5Acα2	GM1	0	0.3
A3	Neu5Acα2-3Galβ1-3GlcNAcβ1-3Galβ1-4Glc-PA	SLe^c	0.5	1.6
A4	Galβ1-3GalNAcβ1-4Galβ1-4Glc-PA 3 3 | | Neu5Acα2 Neu5Acα2	GD1a	0.2	0.3
A5	Galβ1-3GlcNAcβ1-3Galβ1-4Glc-PA 6 | Neu5Acα2	LST-b	0.5	1.2
A6	Neu5Acα2-6Galβ1-4GlcNAcβ1-3Galβ1-4Glc-PA	LST-c	4.9	0.6
A7	Neu5Acα2-3Galβ1-3GlcNAcβ1-3Galβ1-4Glc-PA 6 | Neu5Acα2	$IV^3NeuAc\alpha,III^6NeuAc\alpha\text{-}Lc_4$	0.2	2.3
A8-1	Neu5Acα2-3Galβ1-4GlcNAcβ1-3Galβ1-4Glc-PA 3 | Fucα1	SLe^x	0.1	0.1
A8-2	Neu5Acα2-6Galβ1-3GlcNAcβ1-3Galβ1-4Glc-PA 2 | Fucα1	ST1H	0.1	0
A8-3	Neu5Acα2-6Galβ1-4GlcNAcβ1-3Galβ1-4Glc-PA 2 | Fucα1	ST2H	0.1	0
A12	Galβ1-3GlcNAcβ1-3Galβ1-3GlcNAcβ1-3Galβ1-4Glc-PA 6 | Neu5Acα2	$V^6NeuAc\alpha\text{-}Lc_6$	0	0.4
A9	Neu5Acα2-6Galβ1-4GlcNAcβ1-3Galβ1-3GlcNAcβ1-3Galβ1-4Glc-PA	$VI^6NeuAc\alpha\text{-}_{1,2}Lc_6$	0.2	0
A10	Neu5Acα2-6Galβ1-4GlcNAcβ1-3Galβ1-4GlcNAcβ1-3Galβ1-4Glc-PA 3 | Fucα1	$VI^6NeuAc\alpha,III^3Fuc\alpha\text{-}nLc_6$	2.3	0

neutral				
N1	Galβ1-4Glc-PA	lactose	2.9	4.6
N2	Galα1-4Galβ1-4Glc-PA	Gb_3	3.8	1.9
N3	GalNAcβ1-3Galα1-4Galβ1-4Glc-PA	Gb_4	2.4	0.6
N4	Galβ1-3GlcNAcβ1-3Galβ1-4Glc-PA	Lc_4	26.9	61.4
N5	Galβ1-4GlcNAcβ1-3Galβ1-4Glc-PA	nLc_4	2.5	3.7
N6-1	Fucα1-2Galβ1-3GlcNAcβ1-3Galβ1-4Glc-PA	Type1H	33.5	5.2
N6-2	Fucα1-2Galβ1-4GlcNAcβ1-3Galβ1-4Glc-PA	Type2H	0.3	1.4
N7-1	Galβ1-4GlcNAcβ1-3Galβ1-4Glc-PA 3 | Fucα1	Le^x	5.7	4.9
N7-2	Galβ1-3GlcNAcβ1-3Galβ1-4Glc-PA 4 | Fucα1	Le^a	0.2	0.2
N8	Fucα1-2Galβ1-4GlcNAcβ1-3Galβ1-4Glc-PA 3 | Fucα1	Le^y	4.7	0.4
N9-1	Fucα1-2Galβ1-3GlcNAcβ1-3Galβ1-4Glc-PA 4 | Fucα1	Le^b	0.1	0.1
N9-2	Galβ1-3GlcNAcβ1-3Galβ1-3GlcNAcβ1-3Galβ1-4Glc-PA	Lc_6	1.0	2.8
N13	Galβ1-4GlcNAcβ1-3Galβ1-4GlcNAcβ1-3Galβ1-4Glc-PA	nLc_6	0	1.7
N10-1	Galβ1-4GlcNAcβ1-3Galβ1-4GlcNAcβ1-3Galβ1-4Glc-PA 3 | Fucα1	$V^3Fuc\alpha\text{-}nLc_6$	0.4	0.2
N10-2	Galβ1-4GlcNAcβ1-3Galβ1-3GlcNAcβ1-3Galβ1-4Glc-PA 3 | Fucα1	$V^3Fuc\alpha\text{-}_{1,2}Lc_6$	0.8	1.8
N11	Galβ1-4GlcNAcβ1-3Galβ1-4GlcNAcβ1-3Galβ1-4Glc-PA 2 3 | | Fucα1 Fucα1	$VI^2Fuc\alpha, V^3Fuc\alpha\text{-}nLc_6$	0.1	0
N12	Galβ1-4GlcNAcβ1-3Galβ1-4GlcNAcβ1-3Galβ1-4Glc-PA 3 3 | | Fucα1 Fucα1	$V^3Fuc\alpha, III^3Fuc\alpha\text{-}nLc_6$	1.6	0.5

Lewis-negative individuals, very low levels of Le^a (N7-2) and Le^b (N9-1) were observed in normal epithelial cells of some Lewis-negative individuals (Figure 1A, Table II). This is probably because the highly sensitive methods employed in our study to analyze the oligosaccharide structures facilitated the detection of minute levels of Lewis antigens, which would otherwise be undetectable using conventional procedures. Secondly, a relatively high level of Le^b (N9-1) was found in cancer cells but not normal epithelial cells of some Lewis-negative individuals (Figure 1B, c, Table III). A molecular mechanism by which cancer cells of Lewis-negative individuals synthesize high levels of Le^b is proposed in the Discussion.

Structure of A8-2

Although A8-2 was expressed in three adenocarcinoma cells, it did not match any of the reference compounds on the 2D map

accumulated prior to our studies. MS/MS (MS^2) analysis revealed that A8-2 is monosialylated monofucosylated hexasaccharide GSL having a tetrasaccharide backbone, Hex-HexNAc-Hex-Hex-PA. Hence, four GSLs, SLe^x, SLe^a, $III^6NeuAc\alpha,III^3Fuc\alpha$-$Lc_4$, and ST2H were reasoned to be candidates of A8-2. However, the position of A8-2 on the 2D map did not match any of the four corresponding standards (Figure 2, closed and open circles). A8-2 was digested with neuraminidase from *Arthrobacter ureafaciens* and the products of the digestion subjected to 2D mapping. Analysis of the results showed that the products corresponded to reference compound Type1H but not the other monofucosylated pentasaccharides, Type2H, Le^a, and Le^x (Figure 2, closed and open triangles). From this result, the structure of A8-2 is tentatively predicted to be a sialylated

Table III. Estimated structures of acidic and neutral PA-oligosaccharides from pancreatic cancer and normal pancreatic epithelial cells of case 6 (C, cancer cells; N, normal epithelial cells)

Fraction	Structure	Abbreviation	Ratio (%)	
			C	N
acidic				
A1	Neu5Acα2-3Galβ1-4Glc-PA	GM3	29.0	63.7
A2	Neu5Acα2-8Neu5Acα2-3Galβ1-4Glc-PA	GD3	0.6	0
A11	Galβ1-3GalNAcβ1-4Galβ1-4Glc-PA 3 | Neu5Acα2	GM1	0.5	0
A3	Neu5Acα2-3Galβ1-3GlcNAcβ1-3Galβ1-4Glc-PA	SLe^c	0.5	0.4
A4	Galβ1-3GalNAcβ1-4Galβ1-4Glc-PA 3 3 | | Neu5Acα2 Neu5Acα2	GD1a	1.2	0.4
A6	Neu5Acα2-6Galβ1-4GlcNAcβ1-3Galβ1-4Glc-PA	LST-c	1.5	0
A7	Neu5Acα2-3Galβ1-3GlcNAcβ1-3Galβ1-4Glc-PA 6 | Neu5Acα2	$IV^3NeuAc\alpha,III^6NeuAc\alpha$-$Lc_4$	0.6	1.8
A8-1	Neu5Acα2-3Galβ1-4GlcNAcβ1-3Galβ1-4Glc-PA 3 | Fucα1	SLe^x	0.4	0
A8-2	Neu5Acα2-6Galβ1-3GlcNAcβ1-3Galβ1-4Glc-PA 2 | Fucα1	ST1H	0.3	0
A13	Neu5Acα2-3Galβ1-3GalNAcβ1-3Galα1-4Galβ1-4Glc-PA	$V^3NeuAc\alpha$-Gb_5	0	0.9
A14	Neu5Acα2-3Galβ1-3GalNAcβ1-3Galα1-4Galβ1-4Glc-PA 6 | Neu5Acα2	$V^3NeuAc\alpha$ $IV^6NeuAc\alpha$-Gb_5	0	0.9
neutral				
N1	Galβ1-4Glc-PA	lactose	1.6	0.6
N2	Galα1-4Galβ1-4Glc-PA	Gb_3	2.7	7.9
N3	GalNAcβ1-3Galα1-4Galβ1-4Glc-PA	Gb_4	1.5	1.5
N4	Galβ1-3GlcNAcβ1-3Galβ1-4Glc-PA	Lc_4	0.4	0.5
N5	Galβ1-4GlcNAcβ1-3Galβ1-4Glc-PA	nLc_4	1.0	0.2
N6-1	Fucα1-2Galβ1-3GlcNAcβ1-3Galβ1-4Glc-PA	Type1H	43.3	1.6

N7-1	Galβ1-4GlcNAcβ1-3Galβ1-4Glc-PA 3 | Fucα1	Le^x	3.2	0.7
N14	GalNAcα1-3Galβ1-3GlcNAcβ1-3Galβ1-4Glc-PA 2 | Fucα1	Type1A	3.6	13.3
N8	Fucα1-2Galβ1-4GlcNAcβ1-3Galβ1-4Glc-PA 3 | Fucα1	Le^y	3.1	1.3
N9-1	Fucα1-2Galβ1-3GlcNAcβ1-3Galβ1-4Glc-PA 4 | Fucα1	Le^b	4.9	0
N15	GalNAcα1-3Galβ1-4GlcNAcβ1-3Galβ1-4Glc-PA 2 3 | | Fucα1 Fucα1	ALe^y	0	4.4
N12	Galβ1-4GlcNAcβ1-3Galβ1-4GlcNAcβ1-3Galβ1-4Glc-PA 3 3 | | Fucα1 Fucα1	$V^3Fuc\alpha,III^3Fuc\alpha$-$nLc_6$	0.2	0

form of Fucα1-2Galβ1-3GlcNAcβ1-3Galβ1-4Glc (sialylated type1H). A8-2 was digested with α-fucosidase from bovine kidney, and the product of the digest did not coincide with the position of the any monosialylated pentasaccharide reference compound, SLe^c, LST-b, LST-c, SPG, or GM1 (Figure 2, closed and open diamonds). Linkage position of sialic acid could be determined by the specificity of α2,3-silalidase digestion as described in Materials and methods. Defucosylated product of A8-2 could not be digested with α2,3-sialidase under conditions where the enzyme specifically cleaves the α2-3 linkage (condition 1). However, digestion did occur with α2,3-sialidase under conditions where the enzyme cleaves the α2-3 and α2-6 linkages (condition 2). These results indicate that sialic acid is α2-6 linked to the terminal residue. In addition, the defucosylated desialylated product of A8-2 corresponded to Lc_4 but not other neolacto and ganglio series tetrasaccharides, nLc_4, asialo GM1 on the 2D map (Figure 2, closed and open squares). Hence, the structure of A8-2 is predicted to be NeuAcα2-6(Fucα1-2)Galβ1-3GlcNAcβ1-3Galβ1-4Glc (α2-6 sialylated type1H, abbreviated as ST1H), which has not been reported previously. This structure is consistent with the result from tandem mass analysis (Figure 3). The presence of a fragment ion at *m/z* 622 corresponding to $[NeuAc+dHex+Hex+Na]^+$ in the MS^2 spectra of A8-2 indicates that a fucose and sialic acid residues are linked to the outermost Hex residue. This structure has not been found in any normal colorectal and pancreatic epithelial cells, similar to ST2H.

Discussion

In our previous study, we found a novel GSL in colon cancer, NeuAcα2-6(Fucα1-2)Galβ1-4GlcNAcβ1-3Galβ1-4Glc (ST2H), which is expressed in colorectal and pancreatic cancer cells in about half of the patients, regardless of Lewis type (Korekane et al. 2007). In addition to ST2H, we also found a novel fucoganglioside, NeuAcα2-6(Fucα1-2)Galβ1-3GlcNAcβ1-3Galβ1-4Glc (ST1H). Unlike ST2H, ST1H is believed to accumulate principally in cancer cells from Lewis-negative patients. Although there is a degree of similarity between ST1H and ST2H, the two molecules are fundamentally different. The terminal structure of both GSLs is the same, namely, sialic acid and fucose residue is linked to galactose via an α2-6 linkage and α1-2 linkage, respectively. However, the crucial difference is that the galactose of ST1H and ST2H is linked to GlcNAc via a β1-3 (type1) linkage and β1-4 (type2) linkage, respectively. This structural difference is similar to that between SLe^a and SLe^x, i.e., a sialic acid of both SLe^a and SLe^x is attached to the terminal galactose of Le^a (type 1) and Le^x (type 2) via an α2-3 linkage.

ST1H was found in cancer cells from two of 60 cases of colorectal cancer and one of five cases of pancreatic cancer. The incidence of this moiety in cancer cells appears to be very low. However, taking into consideration the highly likely possibility that this substance is preferentially synthesized in cancer cells of Lewis-negative patients, the incidence cannot be considered low. Specifically, this unique structure was found in two of four colorectal cancer patients and one of two pancreatic cancer patients that were Lewis-negative.

ST1H was not detected in normal colorectal and pancreatic epithelial cells. However, analyzed subjects were limited to cancer and normal epithelial cells of colorectal and pancreatic tissues. In future, the subject of analysis needs to be expanded to other tissues including fetal tissues, hyperplasia, adenoma, and inflammatory tissues to investigate whether ST1H is an oncofetal antigen.

Although the expression level of ST1H is quite low compared with major GSLs, it is nevertheless comparable with that of SLe^x (Tables II and III). Moreover, SLe^x is a well-known tumor-associated carbohydrate antigen, which has

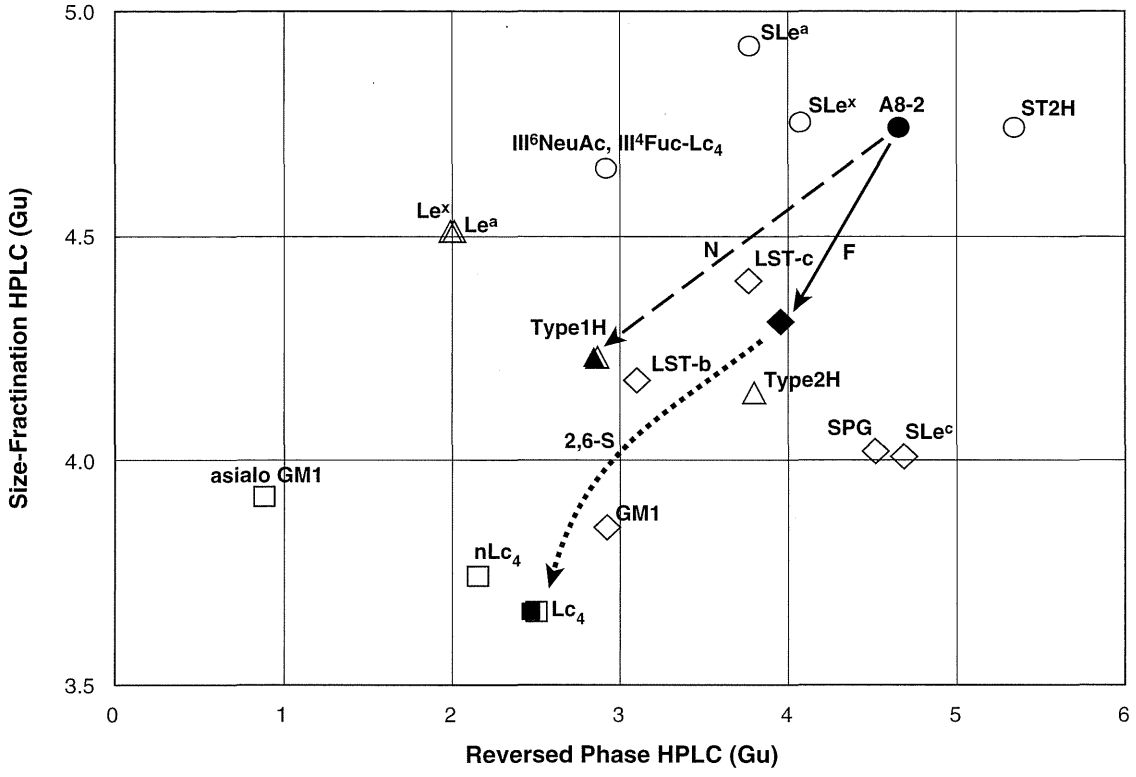

Fig. 2. Sequential digestion of A8-2. Circles, diamonds, triangles, and squares mark the positions of monosialylated monofucosylated hexasaccharides, monosialylated pentasaccharides, monofucosylated pentasaccharides, and tetrasaccharides, respectively. Closed marks indicate A8-2 (closed circle) and change after glycosidase digestion of A8-2 (closed triangle, diamond, and square). Open marks represent the positions of the standard compounds (shown as abbreviations). Lines indicate the direction of the change after glycosidase digestion of A8-2. Glycosidases are shown beside each line. Enzyme abbreviations are: N, α-sialidase (neuraminidase) from *Arthrobacter ureafaciens*; F, α-fucosidase from bovine kidney; 2,6-S, α2,3-sialidase from *Salmonella typhimurium* under conditions where the enzyme digests sialic acid at both α2-3 and α2-6 linkages.

been used as a serum tumor marker, and functions as a ligand for selectins. Therefore, the low level of ST1H expression per se does not necessarily imply an insignificant role in terms of cancer biology.

In addition to identifying novel structures in cancer cells of Lewis-negative individuals, we also found relatively high levels of expression of Le^b (N9-1) in some cancer cells (Figure 1B, c, Table III) even though they are judged to be Lewis-negative. Specifically, no or trace levels of Le^a expression were found in cancer cells and normal epithelial cells, with an undetectable level of CA19-9 in serum, null FUT3 (Lewis) gene and an undetectable level of α1-4 fucosyltransferase activity with Lc_4 (see Results section). We propose that FUT5, but not null FUT3, might be responsible for this reaction. FUT5 has predominantly α1-3 fucosyltransferase activity with type 2 chain acceptors, such as nLc_4 and type 2 disaccharide, and only a very low level of α1-4 fucosyltransferase activity with type 1 chain acceptors, such as Lc_4 and type 1 disaccharide (Weston et al. 1992; Nguyen et al. 1998). However, FUT5 showed comparable levels of α1-4 fucosyltransferase activity with Type 1H to convert to Le^b to FUT3 (Oulmouden et al. 1997). Furthermore, previous work suggests a requirement of Type 1H structures for FUT5 as precursors for type 1 Lewis antigen biosynthesis in cultured cells (Holgersson and Lofling 2006). Hence, even though FUT3 is inactivated, Le^b can be generated by FUT5 in the cells in which Type 1H is dominantly expressed, such as cancer cells of Lewis-negative individuals as described below (N6-1, Figure 1A and B). In agreement with this speculation, cancer cells of case 6 possess undetectable levels of α1-4 fucosyltransferase activity with Lc_4 to form Le^a. However, these cancer cells exhibited quite low, but nevertheless detectable, levels of α1-4 fucosyltransferase activity with Type 1H to form Le^b (data not shown).

Proposed synthetic pathways for the major groups of GSLs in cancer cells and normal epithelial cells are outlined in Figure 4. Based on the findings of our previous work (Misonou et al. 2009) and this study, we believe that the reason that ST1H is likely to be synthesized in cancer cells of Lewis-negative patients is as follows. Le^a and Le^b are the major products, and Type1H and Lc_4 are very minor in normal epithelial cells from Lewis-positive individuals (highlighted by square with thick line, Figure 4). Even though the levels of Le^a and Le^b decrease in carcinogenesis, the levels of Lc_4 and Type1H do not increase and remain quite low. ST1H is scarcely synthesized in cancer and normal epithelial cells from Lewis-positive individuals probably because active Lewis enzyme much prefers to act on Type1H (a precursor of ST1H) over α2-6 sialyltransferase; the pathway would flow to the synthesis of Le^b but not ST1H. α2-6 Sialylated Le^b and Le^a was not detected in our study. This is probably because α2-6 sialyltransferase cannot act on the terminal galactose of a type-1 lactosamine chain when the adjacent GlcNAc is fucosylated. While Lc_4, Type1H, and Type1H derivatives (Type 1A and/

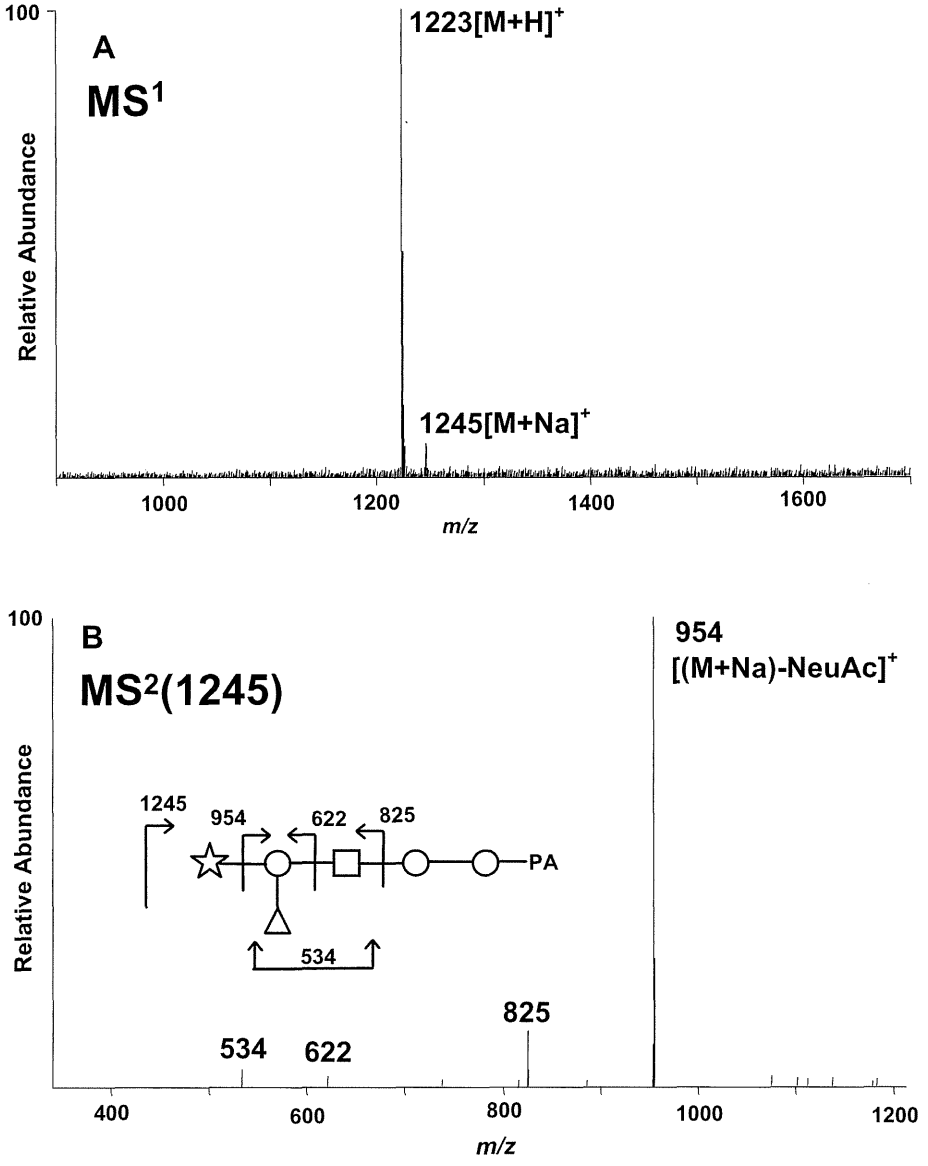

Fig. 3. MS^1 and MS^2 spectra of A8-2. (**A**) MS^1 spectra of A8-2. (**B**) MS^2 spectra of $[M+Na]^+$ precursor ion at *m/z* 1245 detected in MS^1 of panel **A**. Fragment ions with numbered mass values in panel **B** are sodium adduct ions. The MS/MS fragment ions were assigned as shown schematically. Symbols: Hex, open circle; HexNAc, open square; sialic acid, open star; dHex, open triangle.

or B) are the major products, Le^a and Le^b are absent or present at very low levels in normal epithelial cells from Lewis-negative individuals due to the lack of Lewis enzyme activity (highlighted by square with thin line, Figure 4). The common feature of the oligosaccharide structures of the three cancer cells (cases 1, 4, 6) expressing ST1H is that Type 1H is markedly increased to become the most abundant species (Figure 1A and B, N6-1). The marked increase in the level of Type1H from colorectal cancer cells is thought to be due to the elevation of activity of α1-2 fucosyltransferase during carcinogenesis (Misonou et al. 2009). However, the detailed mechanism of the upregulation of Type1H in pancreatic cancer cells of Lewis-negative patients is not clear. Furthermore, augmentation of the activity of α2-6 sialyltransferase during malignant transformation in colorectal cancer cells was demonstrated previously (Misonou et al. 2009). A similar elevation in the activity of α2-6 sialyltransferase in pancreatic cancer cells was also confirmed in our study (data not shown). Hence, the pathway would flow to the synthesis of ST1H in cancer cells from Lewis-negative individuals.

Because Lewis-negative individuals cannot produce the SLe^a epitope (CA19-9 epitope), serum levels of CA19-9 in these individuals is either undetectable or very low (i.e., under 1 U/mL). DU-PAN-2 (SLe^c epitope), which is a precursor structure of SLe^a, is another well-known tumor marker (Figure 4). Hence, measurement of CA19-9 and DU-PAN-2 is recommended to apply for Lewis-positive and Lewis-negative individuals, respectively (Narimatsu et al. 1998) (Figure 4). Both antigenic epitopes are known to be carried on mucins that are secreted into the plasma by cancer cells. Although the unique epitope of ST1H (NeuAcα2-6(Fucα1-2)Galβ1-3GlcNAcβ1-R) was found in GSLs in this study, it is highly possible that the ST1H epitope is also car-

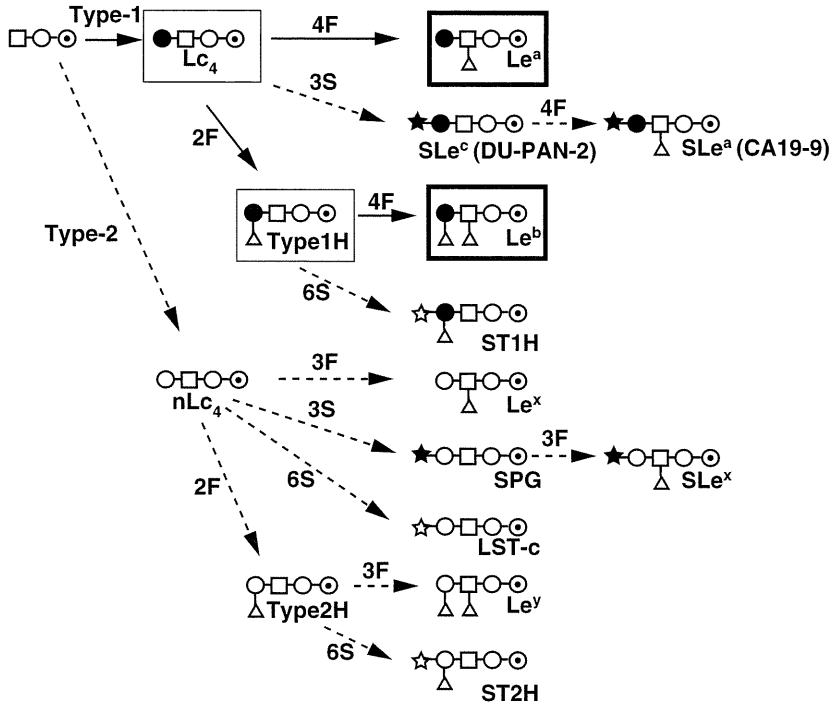

Fig. 4. Proposed synthetic pathways for major groups of GSLs in cancers and normal epithelial cells. Arrows indicate the pathways predominating in normal epithelial cells. Broken arrows indicate the pathways that are increased in carcinogenesis. Abbreviations: 4F, α1-4 fucosylation of GlcNAc (Lewis enzyme activity); 3F, α1-3 fucosylation of GlcNAc; 2F, α1-2 fucosylation of galactose; 3S, α2-3 sialylation of galactose; 6S, α2-6 sialylation of galactose. The structures of GSLs in normal epithelial cells from Lewis-positive individuals are composed of mainly Le^a and Le^b (highlighted by square with thick line). By contrast, the structures of GSLs in normal epithelial cells from Lewis-negative individuals are composed of mainly Lc_4 and Type1H (highlighted by square with thin line). In malignant transformation, the type-2 ratio, α2-3 and/or α2-6 sialylation, and α1-2 fucosylation are increased. These alterations result in increases in the amounts of, or the appearance of, a variety of oligosaccharides, such as Le^x, Le^y, LST-c, SLe^x, and ST2H as type 2 oligosaccharides, Type 1H, SLe^a, SLe^c, and ST1H as type 1 oligosaccharides. Note the difference in composition of type1 oligosaccharides between cancer cells from Lewis-positive and negative individuals, i.e., synthesis of SLe^a is increased in carcinogenesis and SLe^a becomes one of the major components of cancer cells from Lewis-positive individuals. However, SLe^a is not synthesized in cancer cells and normal epithelial cells from Lewis-negative individuals, but the levels of SLe^c and/or ST1H are increased in carcinogenesis. SLe^a epitope (NeuAcα2-3Galβ1-3(Fucα1-4)GlcNAcβ1-R) and SLe^c epitope (NeuAcα2-3Galβ1-3GlcNAcβ1-R) are recognized by CA19-9 and DU-PAN-2 antibodies, respectively. Schemes of representative oligosaccharides are shown. Symbols: open circle with a dot inside, glucose; open circle, galactose (β1-4 linkage, type 2); closed circle, galactose (β1-3 linkage, type 1); open square, GlcNAc; open star, sialic acid (α2-6 linkage); closed star, sialic acid (α2-3 linkage); open triangle, fucose.

ried on the mucins, similar to SLe^a and SLe^c epitopes. Furthermore, the synthetic flow of DU-PAN-2 and ST1H are different; i,e, DU-PAN-2 and ST1H are synthesized by α2-3 sialylation of Lc_4 and α2-6 sialylation of Type1H, respectively (Figure 4). The combination of ST1H and DU-PAN-2 determinants could serve as a highly sensitive tumor marker, especially for Lewis-negative individuals.

Materials and methods

All human specimens were obtained from Osaka Medical Center for Cancer and Cardiovascular Diseases. This study was approved by the Local Ethics Committee of Osaka Medical Center for Cancer and Cardiovascular Diseases. Informed consent was obtained from the patients. The majority of experimental procedures including purification of cancer cells, isolation of GSLs, preparation and separation of PA-oligosaccharides, and mass spectrometry have been reported previously (Misonou et al. 2009). In brief, in order to improve the accuracy of analyses, cancer cells were highly purified from primary lesions of colorectal cancers and pancreatic cancers using the epithelial cell marker, CD326, and magnetic beads. The tissues were dissected into small blocks and incubated in DMEM/F12 medium containing 2 mg/mL collagenase (Sigma-Aldrich, St Louis, MO). The digested cells were resuspended in phosphate-buffered saline containing 2 mM EDTA and 0.5% bovine serum albumin, and CD326 positive cells were positively selected using magnetically labeled microbeads (Miltenyi Biotec GmbH, Bergisch-Gladbach, Germany) according to the manufacturer's protocol.

The neutral and acidic GSLs were extracted from the cells and digested with recombinant endoglycoceramidase II from *Rhodococcus* sp. (Takara Bio Inc. Shiga, Japan) (Ito and Yamagata 1989). Released oligosaccharides were labeled with 2-aminopyridine (Natsuka and Hase 1998).

PA-oligosaccharides were separated on a Shimadzu LC-20A HPLC system equipped with a Waters 2475 fluorescence detector. Normal-phase HPLC was performed on a TSK gel Amide-80 column (0.2 × 25 cm, Tosoh, Tokyo, Japan). The molecular

size of each PA-oligosaccharide is given in glucose units (Gu) based on the elution times of PA-isomaltooligosaccharides. Reversed-phase HPLC was performed on a TSK gel ODS-80Ts column (0.2 × 15 cm, Tosoh). The retention time of each PA-oligosaccharide is given in glucose units based on the elution times of PA-isomaltooligosaccharides. Thus, a given compound on these two columns provides a unique set of Gu (amide) and Gu (ODS) values, which correspond to coordinates of the 2D map. PA-oligosaccharides were analyzed by LC/ESI MS/MS. High-performance liquid chromatography was performed on a Paradigm MS4 equipped with a Magic C18 column (0.2 × 50 mm; Michrome BioResource, Auburn, CA). Mass spectrometry (MS) analyses were performed using a LCQ ion trap mass spectrometer (Thermo Finnigan, San Jose, CA). In the LCQ method file, the LCQ was set to acquire a full MS scan between 400 and 2000 *m/z* followed by MS/MS scans in a data-dependent manner. Protonated ions were subjected to a further product ion scan for nonfucosylated PA-oligosaccharides. However, sodiated ions were subjected to a further product ion scan for fucose containing PA-oligosaccharides because of the following reason: intramolecular fucose rearrangements have been found in the CID spectra of protonated ions (but not in sodiated ions) produced from oligosaccharides derivatized at their reducing termini with aromatic amines, such as 2-aminobenzamide, which may lead to erroneous conclusions about oligosaccharide sequence (Harvey et al. 2002).

Standard PA-oligosaccharides

The structures, abbreviations, and glucose units of authentic PA-oligosaccharides used in this study are listed in Supplemental Table 1, which include PA-oligosaccharides purchased from a commercial source, kindly donated, or prepared during our previous study. Type 1-type 2 hybrid hexasaccharide, Galβ1-4GlcNAcβ1-3Galβ1-3GlcNAcβ1-3Galβ1-4Glc are abbreviated as $_{1,2}Lc_6$, in order of linkage type of the fourth and sixth galactoses.

Glycosidase digestion

Sialyl PA-oligosaccharides were digested with 2 U/mL of α2,3-sialidase from *Salmonella typhimurium* (Takara Bio Inc.) or 2 U/mL of α-sialidase (neuraminidase) from *A. ureafaciens* (Nacalai, Kyoto, Japan) in 100 mM sodium acetate buffer, pH 5.5, for 2 h at 37°C (condition 1). Under these conditions, α2,3-sialidase specifically digests sialic acid α2-3 linked to the terminal residue but not sialic acid with an α2-6 linkage, while *Arthrobacter* α-sialidase digests both linkages independent of the linkage position. However, under conditions using 10 U/mL for 16 h (condition 2), even so-called α2,3-sialidase can hydrolyze sialic acid α2-6 linked to the terminal residue but not sialic acid linked to a non-terminal residue. Hence, we were able to conclude the linkage position of sialic acid using these two enzymes as follows: (1) When sialyl PA-oligosaccharide was cleaved by α2,3-sialidase in condition 1, sialic acid was concluded to be linked to the terminal residue through an α2-3 linkage. (2) When sialyl PA-oligosaccharide was cleaved by α2,3-sialidase in condition 2 but not in condition 1, sialic acid was concluded to be linked to the terminal residue through an α2-6 linkage. (3) When sialyl PA-oligosaccharide was cleaved by *Arthrobacter* α-sialidase in condition 1 but not by α2,3-sialidase in condition 2, sialic acid was concluded to be linked to a non-terminal residue.

PA-oligosaccharides were digested with 10 U/mL of α-fucosidase from bovine kidney (Sigma-Aldrich) in 100 mM sodium acetate buffer, pH 5.5, for 16 h at 37°C. All the reactions were terminated by boiling the solutions for 3 min.

Molecular cloning of Lewis gene (FUT3) alleles

PCR was used to amplify the coding region of the Lewis gene along with the flanking regions immediately 5′- and 3′- of the gene from six patients using the sense primer 5′-GAAACAGGAATAATAGCAGCTCC-3′ and antisense primer 5′-GTTGGCCACAAAGGACTCCAG-3′. Genomic DNA was extracted from normal rectal and pancreatic tissues with the QIAamp DNA Micro Kit (Qiagen, Hilden, Germany). Polymerase chain reactions consisted of 1× PCR buffer (TOYOBO, Osaka, Japan), 1 mM $MgSO_4$, 0.2 mM dNTP each, 0.02 U/μL KOD Plus DNA polymerase (TOYOBO), 0.5 μM each of sense and antisense primer, and Genomic DNA in a 20-μL reaction volume. The PCR program included hot start at 94°C for 2 min, followed by 35 cycles with 15 s at 94°C, 30 s at 56°C, and 1 min at 68°C. The PCR products were sequenced directly in their entirety using the BigDye Terminator Cycle Sequencing Kit (version 3.1; Applied Biosystems, Foster City, CA) with the 3100 Genetic Analyzer (Applied Biosystems). Furthermore, PCR products from a heterozygote were ligated into pTA2 TA-cloning vector (TOYOBO) according to the manufacturer's protocol. Positive clones were selected by blue-white screening, and both strands of their inserts were sequenced. We used oligonucleotides corresponding to flanking plasmid sequences and primers corresponding to internal sequences of the wild-type FUT3.

Lewis enzyme (α1-4 fucosyltransferase) activity

Highly purified cancer and normal epithelial cells were washed with phosphate-buffered saline, resuspended in 50 μL of 1% Triton X100, 20 mM HEPES (pH 7.4) and then subjected to sonication to obtain the cell homogenate. After centrifugation at 12,000 × *g* for 10 min, the supernatants were used as enzyme sources. The supernatants (1 μL) were assayed for fucosyltransefarse activities in 50 mM cacodylate buffer, pH 6.5, 5 mM ATP, 25 mM $MnCl_2$, 10 mM L-fucose, 75 μM GDP-fucose, and 1 mM PA-Lc_4 (a total volume of 5 μL). The reaction mixtures were incubated at 37°C for 2 h and terminated by boiling for 3 min. After centrifugation at 12,000 × *g* for 10 min, the supernatants were subjected to size fractionation HPLC.

Supplementary data

Supplementary data mentioned in the text is available to subscribers in *Glycobiology* online.

Acknowledgments

This study was supported by the Program for Promotion of Fundamental Studies in Health Sciences of the National Institute of Biomedical Innovation (NIBIO) and Grant-in-Aid from Japan Foundation for Applied Enzymology. We thank Dr. Shunji Natsuka and Dr. Koichi Honke for useful discussions and critical comments on the manuscript.

Abbreviations

GSL, glycosphingolipids; Gu, glucose units; SLe^a, sialyl Le^a; SLe^x, sialyl Le^x; ST1H, α2-6 sialylated type1H; ST2H, α2-6 sialylated type 2H.

References

Elmgren A, Mollicone R, Costache M, Borjeson C, Oriol R, Harrington J, Larson G. 1997. Significance of individual point mutations, T202C and C314T, in the human Lewis (FUT3) gene for expression of Lewis antigens by the human alpha(1, 3/1, 4)-fucosyltransferase, Fuc-TIII. *J Biol Chem.* 272(35):21994–21998.

Fukuda M. 1996. Possible roles of tumor-associated carbohydrate antigens. *Cancer Res.* 56(10):2237–2244.

Hakomori S. 1989. Aberrant glycosylation in tumors and tumor-associated carbohydrate antigens. *Adv Cancer Res.* 52:257–331.

Hakomori S. 1996. Tumor malignancy defined by aberrant glycosylation and sphingo(glyco)lipid metabolism. *Cancer Res.* 56(23):5309–5318.

Hakomori S. 1999. Antigen structure and genetic basis of histo-blood groups A, B and O: their changes associated with human cancer. *Biochim Biophys Acta.* 1473(1):247–266.

Hakomori S. 2002. Glycosylation defining cancer malignancy: new wine in an old bottle. *Proc Natl Acad Sci USA.* 99(16):10231–10233.

Harvey DJ, Mattu TS, Wormald MR, Royle L, Dwek RA, Rudd PM. 2002. "Internal residue loss": rearrangements occurring during the fragmentation of carbohydrates derivatized at the reducing terminus. *Anal Chem.* 74(4):734–740.

Holgersson J, Lofling J. 2006. Glycosyltransferases involved in type 1 chain and Lewis antigen biosynthesis exhibit glycan and core chain specificity. *Glycobiology.* 16(7):584–593.

Ito M, Yamagata T. 1989. Purification and characterization of glycosphingolipid-specific endoglycosidases (endoglycoceramidases) from a mutant strain of *Rhodococcus* sp. Evidence for three molecular species of endoglycoceramidase with different specificities. *J Biol Chem.* 264(16):9510–9519.

Kannagi R, Izawa M, Koike T, Miyazaki K, Kimura N. 2004. Carbohydrate-mediated cell adhesion in cancer metastasis and angiogenesis. *Cancer Sci.* 95(5):377–384.

Korekane H, Tsuji S, Noura S, Ohue M, Sasaki Y, Imaoka S, Miyamoto Y. 2007. Novel fucogangliosides found in human colon adenocarcinoma tissues by means of glycomic analysis. *Anal Biochem.* 364(1):37–50.

Kudo T, Iwasaki H, Nishihara S, Shinya N, Ando T, Narimatsu I, Narimatsu H. 1996. Molecular genetic analysis of the human Lewis histo-blood group system. II. Secretor gene inactivation by a novel single missense mutation A385T in Japanese nonsecretor individuals. *J Biol Chem.* 271(16):9830–9837.

Kukowska-Latallo JF, Larsen RD, Nair RP, Lowe JB. 1990. A cloned human cDNA determines expression of a mouse stage-specific embryonic antigen and the Lewis blood group alpha(1, 3/1, 4)fucosyltransferase. *Genes Dev.* 4(8):1288–1303.

Misonou Y, Shida K, Korekane H, Seki Y, Noura S, Ohue M, Miyamoto Y. 2009. Comprehensive clinico-glycomic study of 16 colorectal cancer specimens: elucidation of aberrant glycosylation and its mechanistic causes in colorectal cancer cells. *J Proteome Res.* 8(6):2990–3005.

Mollicone R, Reguigne I, Kelly RJ, Fletcher A, Watt J, Chatfield S, Aziz A, Cameron HS, Weston BW, Lowe JB. 1994. Molecular basis for Lewis alpha(1, 3/1, 4)-fucosyltransferase gene deficiency (FUT3) found in Lewis-negative Indonesian pedigrees. *J Biol Chem.* 269(33): 20987–20994.

Narimatsu H, Iwasaki H, Nakayama F, Ikehara Y, Kudo T, Nishihara S, Sugano K, Okura H, Fujita S, Hirohashi S. 1998. Lewis and secretor gene dosages affect CA19-9 and DU-PAN-2 serum levels in normal individuals and colorectal cancer patients. *Cancer Res.* 58(3):512–518.

Narimatsu H, Iwasaki H, Nishihara S, Kimura H, Kudo T, Yamauchi Y, Hirohashi S. 1996. Genetic evidence for the Lewis enzyme, which synthesizes type-1 Lewis antigens in colon tissue, and intracellular localization of the enzyme. *Cancer Res.* 56(2):330–338.

Natsuka S, Hase S. 1998. Analysis of *N*- and *O*-glycans by pyridylamination. *Methods Mol Biol.* 76:101–113.

Nguyen AT, Holmes EH, Whitaker JM, Ho S, Shetterly S, Macher BA. 1998. Human alpha1, 3/4-fucosyltransferases. I. Identification of amino acids involved in acceptor substrate binding by site-directed mutagenesis. *J Biol Chem.* 273(39):25244–25249.

Nishihara S, Hiraga T, Ikehara Y, Iwasaki H, Kudo T, Yazawa S, Morozumi K, Suda Y, Narimatsu H. 1999. Molecular behavior of mutant Lewis enzymes in vivo. *Glycobiology.* 9(4):373–382.

Nishihara S, Narimatsu H, Iwasaki H, Yazawa S, Akamatsu S, Ando T, Seno T, Narimatsu I. 1994. Molecular genetic analysis of the human Lewis histo-blood group system. *J Biol Chem.* 269(46):29271–29278.

Oulmouden A, Wierinckx A, Petit JM, Costache M, Palcic MM, Mollicone R, Oriol R, Julien R. 1997. Molecular cloning and expression of a bovine alpha (1, 3)-fucosyltransferase gene homologous to a putative ancestor gene of the human FUT3-FUT5-FUT6 cluster. *J Biol Chem.* 272(13):8764–8773.

Weston BW, Nair RP, Larsen RD, Lowe JB. 1992. Isolation of a novel human alpha (1, 3)fucosyltransferase gene and molecular comparison to the human Lewis blood group alpha (1, 3/1, 4)fucosyltransferase gene. Syntenic, homologous, nonallelic genes encoding enzymes with distinct acceptor substrate specificities. *J Biol Chem.* 267(6):4152–4160.

Yazawa S, Nishihara S, Iwasaki H, Asao T, Nagamachi Y, Matta KL, Narimatsu H. 1995. Genetic and enzymatic evidence for Lewis enzyme expression in Lewis-negative cancer patients. *Cancer Res.* 55(7):1473–1478.

Clinica Chimica Acta 406 (2009) 179–180

Contents lists available at ScienceDirect

Clinica Chimica Acta

journal homepage: www.elsevier.com/locate/clinchim

Letter to the Editor

Effects of the time intervals between venipuncture and serum preparation for serum peptidome analysis by matrix-assisted laser desorption/ionization time-of-flight mass spectrometry

Dear Editor:

With the recent advances in proteomics technologies, protein and peptide biomarker discovery is now one of the major applications of proteome research [1,2]. Profiling methods based on mass spectrometry (MS) such as surface enhanced laser desorption/ionization time-of-flight (SELDI-TOF) MS and matrix-assisted laser desorption ionization time-of-flight (MALDI-TOF) MS analysis of blood samples are promising tools for biomarker discovery [3,4].

However, several studies indicated that preanalytical factors have significant effects on the results of blood proteome analysis [5–13]. Appropriate specimen collection and handling towards the standardization of parameters for plasma proteome samples has been established by the HUPO plasma proteome project [14]. On the other hand, appropriate conditions for serum sample processing for peptidome analysis has not yet been fully established.

Among various preanalytical factors tested so far, the time intervals between venipuncture and serum separation (clotting time) could have significant effects on the results [11–13]. We determined in detail the effects of the clotting time on the profiles of serum peptidome analyses. Other preanalytical factors related to clinical laboratory such as freezing methods and the effects of freeze–thaw cycles were also assessed.

α-Cyano-4-hydroxycinnamic acid (CHCA) matrix (Bruker Daltonics, Bremen, Germany) solution was diluted as 0.3 g/l in ethanol:acetone (2:1) solution. Acetone and ethanol were HPLC-grade and were from Wako Pure Chemical Industries (Osaka, Japan). We collected serum samples from a total of 7 healthy volunteers (5 males, 2 females, 29–47 y) with written informed consent. The sample collection, handling and storage conditions were defined according to the specific experimental conditions as described in the text. Otherwise, serum samples were collected as follows; blood samples were collected in vacutainer tubes (InsepakII, Sekisui Kagaku Kogyo, Tokyo, Japan). After collection, the samples were allowed to clot at room temperature for 1 h and then sera were separated by centrifugation at 1500 ×*g* for 10 min at 4 °C. Sera were divided into aliquots in SUMILON Proteosave® SS 1.5 ml tube (Sumitomo Bakelite, Tokyo, Japan) and were stored at −80 °C until analysis.

Serum sampling and handling procedures for the analysis of each preanalytical factor were as follows. Except for the experiments to test the effects of various clotting time for serum protein profiles, serum samples were obtained by centrifugation 1 h after venipuncture. 1) For the assessment of the effects of clotting time, sera were collected 15 min, 30 min, 1, 2, 4, and 6 h after venipuncture in 4 subjects. 2) For the assessment of the effects of freezing methods, serum samples obtained from 3 subjects were frozen with liquid nitrogen or directly in freezers (−80 or −20 °C). The frozen samples were thawed on ice after one week and were subjected to analyses. 3) For the assessment of the effects of freeze/thaw cycles, 3serum samples were frozen directly in the −80 °C deep freezer and were then thawed on ice. One to seven freeze/thaw cycles were performed.

We employed magnetic beads with C8-hydrophobic interaction chromatography (C8), weak cation exchange (WCX) or immobilized metal affinity chromatography (IMAC-Cu) resin and performed serum peptidome fractionation with these 3 magnetic beads according to the manufacturer's protocol. A portion of the eluted sample (1 μl) was mixed with 10 μl of CHCA matrix. Then, 0.8 μl of the resulting mixture was spotted onto AnchorChip™ target plate, and crystallized. Every samples were duplicated, and quadricate spotting were performed for one elution. For data analysis, spectra from these eight spots were averaged. All these procedures were performed automatically with ClinProtRobot (Bruker Daltonics).

The AnchorChip™ target plate was placed in an AutoflexII TOF/TOF MS (Bruker Daltonics) controlled by Flexcontrol™2.4 software (Bruker Daltonics). The instrument is equipped with a 337 nm nitrogen laser, delayed-extraction electronics, and a 25 Hz digitizer. All acquisitions were generated by an automated acquisition method included in the instrument software and based on averaging 1000 randomized shots. The acquisition laser power was set between 20 and 35%. Spectra were acquired in positive linear mode, in the mass range of 600–10,000 Da. Peak clusters were completed using second pass peak section (signal to noise ratio >5). Then, we analyzed serum peptidome data with ClinProtools 2.1 software (Bruker Daltonics).

Time courses of the relative intensity of each peak appear to be categorized as 3 patterns as indicated in Fig. 1A (Types A–C). It was possible to classify all the peaks obtained into these 3 types as summarized in Fig. 1B. In analyses with WCX and C8 beads, more than half of the peaks were categorized as type C. On the other hand, type B was most common when IMAC-Cu bead were used.

3 different freezing methods, freezing in liquid nitrogen, freezing in freezer (−20 °C, −80 °C) were compared in 3 different samples. The relative intensities of each peak obtained under these 3 conditions were quite consistent when serum samples were frozen in liquid nitrogen and −80 °C freezer.

Effects of freeze/thaw cycles on serum peptide profiles were also assessed in 3 different samples. CVs of relative intensities of each peak among various freeze/thaw cycles were obtained. Numbers of peaks in which CV was >20% were few when the freeze/thaw was within 2 cycles.

Clotting time was by far the most influential preanalytical factor tested in this study. Time-dependent changes of serum proteome profiles based on magnetic bead separation and MALDI-TOF MS before centrifugation of the blood samples have been described previously [11–13]. Most previous reports, however, looked at only selected peaks in blood samples in contrast to the present study in which the effects of clotting time on all the detectable peptide peaks were evaluated. We found the effects of clotting time on time courses of the relative intensity of each peak can be categorized into 3 groups. To give an example, the 5.9 kDa peptide that we previously reported as a promising biomarker of excessive alcohol consumption [15–17] was categorized as type C, the most stable type. In the process of biomarker discovery by serum

0009-8981/$ - see front matter
doi:10.1016/j.cca.2009.06.007

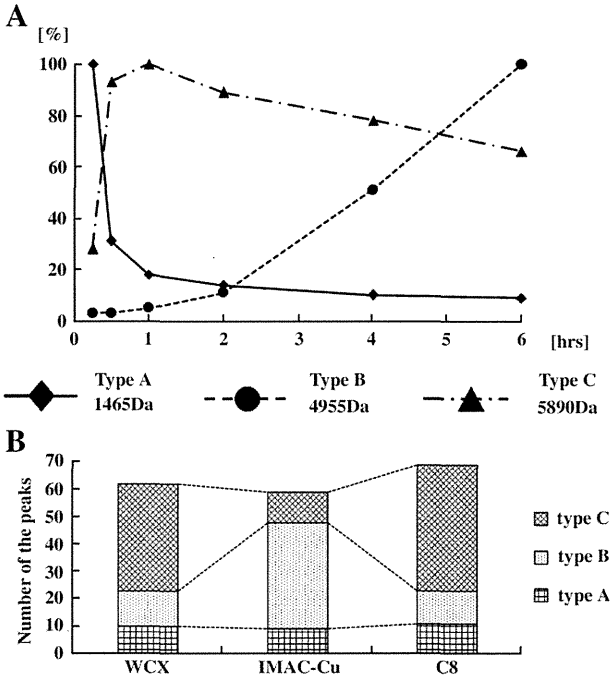

Fig. 1. Time courses of the intensities of serum peptide peaks between venipuncture and serum separation. (A) In type A, the relative intensities of the peak decrease in a time-dependent manner after venipuncture. On the other hand, the relative intensities increase in type B. In type C, they increase remarkably during the first 30 min, but are relatively stable thereafter. (B) The number of peaks categorized as types A–C.

peptidome analyses, one may have to consider the time course of the marker candidate after venipuncture and to know in which type of the patterns the particular marker can be categorized.

The number of peaks detectable by the ClinProt™ system was largest when serum samples were obtained around 60 min after venipunctures. It will be reasonable to set time intervals of 60 min between venipuncture and serum separation for efficient marker discovery by serum peptidome analyses.

The ideal way to freeze and store serum samples is to use liquid nitrogen and its container. It is not necessarily practical to use liquid nitrogen on a routine basis; some alternatives are required to conduct multi-center validation study. As long as short-term storage is concerned, our data indicated that serum proteome profiles obtained by samples frozen and stored at −80 °C were comparable to those obtained by samples frozen and stored in liquid nitrogen. Also, it was shown that freezing and thawing sample more than twice should be avoided, suggesting that serum samples for serum peptidome analyses have to be initially divided into aliquots.

Careful sample collection and handling procedures should have profound impact on serum peptidome patterns, especially in inter-laboratory or multi-center studies. The results of this study indicate that clotting time is a critical preanalytical factor, and that serum peptide peaks can be categorized into 3 groups in terms of their time courses. It is essential to know to which group each candidate peak belongs when planning and conducting validation studies.

References

[1] Righetti PG, Castagna A, Antonucci F, et al. Proteome analysis in the clinical chemistry laboratory: myth or reality? Clin Chim Acta 2005;357:123–39.
[2] Colantonio DA, Chan DW. The clinical application of proteomics. Clin Chim Acta 2005;357:151–8.
[3] Diamandis EP. Mass spectrometry as a diagnostic and a cancer biomarker discovery tool: opportunities and potential limitations. Mol Cell Proteomics 2004;3:367–78.
[4] Hortin GL. The MALDI-TOF mass spectrometric view of the plasma proteome and peptidome. Clin Chem 2006;52:1223–37.
[5] Banks RE, Stanley AJ, Cairns DA, et al. Influences of blood sample processing on low-molecular-weight proteome identified by surface-enhanced laser desorption/ionization mass spectrometry. Clin Chem 2005;51:1637–49.
[6] Albrethsen J, Bogebo R, Olsen J, Raskov H, Gammeltoft S. Preanalytical and analytical variation of surface-enhanced laser desorption-ionization time-of-flight mass spectrometry of human serum. Clin Chem Lab Med 2006;44:1243–52.
[7] Timms JF, Arslan-Low E, Gentry-Maharaj A, et al. Preanalytic influence of sample handling on SELDI-TOF serum protein profiles. Clin Chem 2007;53:645–56.
[8] West-Norager M, Kelstrup CD, Schou C, Hogdall EV, Hogdall CK, Heegaard NH. Unravelling in vitro variables of major importance for the outcome of mass spectrometry-based serum proteomics. J Chromatogr B Analyt Technol Biomed Life Sci 2007;847:30–7.
[9] Yi J, Kim C, Gelfand CA. Inhibition of intrinsic proteolytic activities moderates preanalytical variability and instability of human plasma. J Proteome Res 2007;6:1768–81.
[10] Luque-Garcia JL, Neubert TA. Sample preparation for serum/plasma profiling and biomarker identification by mass spectrometry. J Chromatogr A 2007;1153:259–76.
[11] West-Nielsen M, Hogdall EV, Marchiori E, Hogdall CK, Schou C, Heegaard NH. Sample handling for mass spectrometric proteomic investigations of human sera. Anal Chem 2005;77:5114–23.
[12] Hsieh SY, Chen RK, Pan YH, Lee HL. Systematical evaluation of the effects of sample collection procedures on low-molecular-weight serum/plasma proteome profiling. Proteomics 2006;6:3189–98.
[13] Baumann S, Ceglarek U, Fiedler GM, Lembcke J, Leichtle A, Thiery J. Standardized approach to proteome profiling of human serum based on magnetic bead separation and matrix-assisted laser desorption/ionization time-of-flight mass spectrometry. Clin Chem 2005;51:973–80.
[14] Rai AJ, Gelfand CA, Haywood BC, et al. HUPO Plasma Proteome Project specimen collection and handling: towards the standardization of parameters for plasma proteome samples. Proteomics 2005;5:3262–77.
[15] Nomura F, Tomonaga T, Sogawa K, et al. Identification of novel and downregulated biomarkers for alcoholism by surface enhanced laser desorption/ionization-mass spectrometry. Proteomics 2004;4:1187–94.
[16] Sogawa K, Itoga S, Tomonaga T, Nomura F. Diagnostic values of surface-enhanced laser desorption/ionization technology for screening of habitual drinkers. Alcohol Clin Exp Res 2007;31:S22–6.
[17] Nomura F, Tomonaga T, Sogawa K, Wu D, Ohashi T. Application of proteomic technologies to discover and identify biomarkers for excessive alcohol consumption: a review. J Chromatogr B Analyt Technol Biomed Life Sci 2007;855:35–41.

Hiroshi Umemura*
Masahiko Nezu
Mamoru Satoh
Asako Kimura
Takeshi Tomonaga
Fumio Nomura
Department of Molecular Diagnosis, Graduate School of Medicine, Chiba University, Japan
*Corresponding author. Department of Molecular Diagnosis, Graduate School of Medicine, Chiba University, 1-8-1 Inohana, Chuo-ku, Chiba City, Chiba, Japan 260-8670.
Tel.: +81 43 226 2167; fax: +81 43 226 2169.
E-mail address: UGN11252@nifty.com (H. Umemura).

Yoshio Kodera
Department of Physics, School of Science, Kitasato University, Japan

23 March 2009

ALCOHOLISM: CLINICAL AND EXPERIMENTAL RESEARCH

Vol. 35, No. 2
February 2011

Increased Serum Levels of Pigment Epithelium-Derived Factor by Excessive Alcohol Consumption—Detection and Identification by a Three-Step Serum Proteome Analysis

Kazuyuki Sogawa, Yoshio Kodera, Mamoru Satoh, Yusuke Kawashima, Hiroshi Umemura, Katsuya Maruyama, Hirotaka Takizawa, Osamu Yokosuka, and Fumio Nomura

Background: The search for biological markers of alcohol abuse is of continual interest in experimental and clinical alcohol research. We previously used gel-free proteome analysis methods such as the ProteinChip® system and the ClinProt™ system to search for new serum markers for alcoholism and found several novel marker candidates. As serum contains thousands of proteins and peptides that are present in a large dynamic concentration, depletion of the abundant proteins and further fractionation of the remainder is necessary to get into the deep proteome. We recently described a simple and highly reproducible three-step method for identifying potential disease-marker candidates among the low-abundance serum proteins.

Methods: Two serum samples—one on admission and one after 8 weeks of abstinence—were obtained from 8 patients with alcohol dependency. The samples were subjected to a three-step serum proteome analysis. The steps were the following: first, immunodepletion of the 6 most abundant proteins; second, fractionation using reverse-phase high-performance liquid chromatography; and third, separation using one-dimensional sodium dodecyl sulfate polyacrylamide gel electrophoresis (SDS–PAGE). Differences revealed by protein staining were further confirmed by Western blotting and by enzyme-linked immunosorbent assays (ELISA).

Results: Three-step serum proteome analysis revealed that the serum levels of 5 proteins, alpha2-HS glycoprotein, apolipoprotein A-I, glutathione peroxidase 3, heparin cofactor II, and pigment epithelial-derived factor (PEDF), were significantly greater on admission than after 8 weeks of abstinence. We focused on PEDF because alterations in its levels in alcoholic subjects are not well known. Western blotting and ELISA confirmed the upregulation of PEDF. Serum PEDF levels were significantly greater in moderate to heavy habitual drinkers (14.2 ± 7.7 μg/ml) than in healthy subjects without a drinking history (5.5 ± 3.0 μg/ml) ($p < 0.001$). The serum PEDF levels in subjects with nonalcoholic chronic liver diseases were comparable to the PEDF levels in healthy subjects.

Conclusion: Three-step serum proteome analysis reveals that excessive alcohol drinking increases the PEDF level.

Key Words: Alcoholism, Pigment Epithelial-Derived Factor, Proteomics, Serum.

EXCESSIVE ALCOHOL CONSUMPTION causes alcoholism and alcoholic liver diseases and aggravates many common medical problems such as hypertension, diabetes mellitus, and gout. Although the primary strategy for detecting heavy drinking relies on self-reporting, heavy drinkers tend to underestimate their alcohol consumption. This leads to an underdiagnosis of hazardous alcohol use and related disorders (Alling et al., 2005). Therefore, the search for biological markers of alcohol abuse is of continual interest in experimental and clinical alcohol research (Hannuksela et al., 2007; Niemela, 2007; Nomura et al., 2007).

We previously used the ProteinChip® system to search for new serum markers of alcoholism and found several novel marker candidates (Nomura et al., 2004). Of these markers, a 5.9-kDa peptide (which is a fragment of the fibrinogen alpha chain) with an *m/z* of 5890 was useful in detecting gamma-glutamyltransferase (GGT) nonresponders in male subjects seeking a medical checkup (Sogawa et al., 2007). More recently, we used the ClinProt™ system (Bruker Daltonics, Bremen, Germany; consisting of a combination of beads processing and matrix-assisted laser desorption/ionization

From the Clinical Proteomics Research Center (KS, YK, MS, YK, FN), Chiba University Hospital, Chiba, Japan; Department of Physics (YK), School of Science, Kitasato University, Kanagawa, Japan; Department of Molecular Diagnosis (HU, FN), Graduate School of Medicine, Chiba University, Chiba, Japan; National Hospital Organization Kurihama Alcoholism Center (KM), Kanagawa, Japan; Kashiwado Clinic in Port-Square (HT), Kashiwado Memorial Foundation, Chiba, Japan; and Division of Gastroenterology (OY), Chiba University Hospital, Chiba, Japan.

Received for publication April 26, 2010; accepted July 18, 2010.

Reprint requests: Fumio Nomura, MD, PhD, Department of Molecular Diagnosis, Graduate School of Medicine, Chiba University, 1-8-1 Inohana, Chuo-ku, Chiba City, Chiba 260-8670, Japan; Fax: +81-43-226-2324; E-mail: fnomura@faculty.chiba-u.jp

DOI: 10.1111/j.1530-0277.2010.01336.x

time-of-flight mass spectroscopy [MALDI-TOF MS]) to facilitate close analysis of serum peptide markers not detectable by the ProteinChip® system. We found 4 other peaks as candidate peptide markers (Sogawa et al., 2009).

A technical challenge in serum proteome analysis is that serum contains thousands of proteins and peptides that are present in a large dynamic concentration. Indeed, 22 abundant proteins such as albumin, immunoglobulins, and transferrin constitute up to 99% of the protein content of plasma (Anderson and Anderson, 2002; Tirumalai et al., 2003). Depletion of these abundant proteins and further fractionation of samples will be necessary in future proteomic studies searching for low-abundance serum proteins or peptides.

We recently described a simple and highly reproducible three-step method for identifying potential disease-marker candidates among the low-abundance serum proteins (Kawashima et al., 2009). Using this method, we successfully identified 3 proteins, including YKL-50, as promising biomarkers of sepsis (Hattori et al., 2009). The three steps are the following: first, immunodepletion of the abundant proteins; second, fractionation using reverse-phase high-performance liquid chromatography (HPLC); and third, one-dimensional sodium dodecyl sulfate polyacrylamide gel electrophoresis (SDS–PAGE). In this study, we applied this three-step proteome analysis method to gain more insight into the alterations of serum proteins resulting from excessive alcohol consumption. We detected and identified increased pigment epithelial-derived factor (PEDF) serum levels after excessive alcohol consumption.

MATERIALS AND METHODS

Patients

Sequential serum samples were obtained from patients with alcohol dependency on admission and after 8 weeks of abstinence. The patients were diagnosed in accordance with the DSM IV criteria (American Psychiatric Association, 1994) and admitted to the National Hospital Organization Kurihama Alcoholism Center (Kanagawa, Japan). All of the patients consumed more than 100 g of alcohol per day for more than 10 years until the day of hospitalization.

A total of 120 patients with biopsy-proven nonalcoholic liver diseases were included. In this group, 20 patients had chronic hepatitis B; 20 patients had liver cirrhosis because of hepatitis B virus (HBV) infection; 20 patients had chronic hepatitis C; 20 patients had liver cirrhosis because of hepatitis C virus (HCV) infection; 20 patients had autoimmune hepatitis; and 20 patients had primary biliary cirrhosis.

Blood samples were also obtained from 60 apparently healthy subjects with various drinking habits who visited the Kashiwado Clinic in Port-Square of Kashiwado Memorial Foundation (Chiba, Japan) for their annual medical checkup. All subjects were administered a detailed questionnaire concerning the amount of alcoholic beverages consumed (calculated as grams of ethanol per day), the duration of drinking, and the frequency of drinking. Twenty nondrinkers, 20 light drinkers (less than 40 g/d), and 20 heavy drinkers (more than 80 g/d) were randomly selected from subjects who sought a medical checkup. These subgroups were defined by the criteria reported by Conigrave and colleagues (2002).

The demographic data of the subjects studied are presented in Table 1.

All the serum samples were collected, processed in a protocol that we previously described (Umemura et al., 2009), and stored at −80°C in aliquots until analysis. All of the subjects provided written informed consent, and the Ethics Committee of Chiba University School of Medicine approved this study.

The Removal of High-Abundance Proteins From the Serum Samples

The first step of the three-step analysis involved removing the 6 major serum proteins—albumin, immunoglobulin G, alpha-1-antitrypsin, immunoglobulin A, transferrin, and haptoglobin—by passing them through a commercially available immunoaffinity column, the Multi Affinity Removal column (Agilent Technologies Inc., Santa Clara, CA). Twenty-five microliters of serum was diluted to 75 μL with a loading buffer (Agilent Technologies Inc.) and spin-filtered (0.22 μm) for 30 min at 13,000 rpm and 4°C. One hundred microliters of each sample was injected from an autosampler cooled to 4°C. Depletion was performed at room temperature on a Shimadzu LC10A VP HPLC system (Shimadzu Co., Kyoto, Japan), using the following program: 9 min at 100% eluent A (Agilent Technologies Inc.) at 0.25 ml/min; 3.5 min at 100% eluent B (Agilent Technologies Inc.) at 1.0 ml/min; and then 7.5 min at 100% eluent A at 1.0 ml/min. Based on the chromatogram, which was recorded by measuring the absorbance of the eluate at 280 nm, the flow-through fractions eluted at a retention time between 2.5 min and 6.5 min were collected in eight 0.125 mL aliquots (for a total volume of 1.0 ml). Using Vivaspin 2 Polyethersulfone spin concentrators (molecular weight cutoff at 10 kDa; Vivascience, Hannover, Germany), the flow-through fractions were combined and concentrated by centrifugal ultrafiltration to a total volume of 80 μL. The concentrated sample solution was stored at −80°C until use.

Table 1. Demographic Data of Subjects Studied

Experimental diseases (number of patients)	Sex (M/F)	Age (mean ± SD)	Alcohol consumption (mean ± SD g/d)
Alcohol dependency (n = 20)	20/0	52.8 ± 11.9	201.3 ± 57.3
Healthy volunteers			
Nondrinkers (n = 20)	20/0	50.9 ± 9.0	–
Low-risk drinkers (n = 20)	20/0	50.0 ± 5.3	30.0 ± 6.2
High-risk drinkers (n = 20)	20/0	50.4 ± 6.5	107.5 ± 35.2
Nonalcoholic liver disease			
Hepatitis B virus infection			
Chronic hepatitis (n = 20)	10/10	49.2 ± 14.6	–
Liver cirrhosis (n = 20)	10/10	61.6 ± 9.3	–
Hepatitis C virus infection			
Chronic hepatitis (n = 20)	12/8	63.9 ± 14.6	–
Liver cirrhosis (n = 20)	12/8	69.4 ± 8.5	–
Autoimmune hepatitis (n = 20)	4/16	61.7 ± 15.3	–
Primary biliary cirrhosis (n = 20)	4/16	63.2 ± 8.3	–

Reverse-Phase High-Performance Liquid Chromatography

The second step of the three-step analysis involved subjecting the concentrated flow-through fractions (75 μL) to the Intrada WP-RP column (Imtakt, Kyoto, Japan), which was attached to an HPLC system (NANOSPACE SI-2 system; Shiseido Fine Chemicals, Tokyo, Japan). We conducted chromatography, as previously described (Kawashima et al., 2009). Each fraction was dried in a centrifugal vacuum concentrator and stored at −80°C for subsequent SDS–PAGE analysis.

SDS–PAGE Analysis

The third step of the three-step analysis involved subjecting each HPLC fraction to SDS–PAGE. The lyophilized samples of the HPLC fractions were dissolved in a PAGE sample buffer (pH 6.8; 50 mM Tris–HCl, 50 mM dithiothreitol, 0.5% SDS and 10% glycerol). The solution was then analyzed using SDS–PAGE (Perfect NT Gel W, 10 to 20% acrylamide, 20 wells; DRC Co., Ltd., Tokyo, Japan) in accordance with the manufacturer's protocol. The gel was stained with Coomassie brilliant blue (CBB) (PhastGel Blue R; GE Healthcare, Little Chalfont, UK). TotalLab TL120 software v2006 (Shimadzu Co.) quantified the intensity of each protein band, and the intensity was used as an index of the level of protein expression. The protein bands were excised from the gel; in-gel tryptic digestion was performed and the protein was identified, as we previously described (Hattori et al., 2009).

Western Blotting

The protein extracts were separated by electrophoresis on 10 to 20% gradient gels (DRC Co., Ltd.). The proteins were transferred to polyvinylidene fluoride membranes (Millipore Corporate Headquarters, Billerica, MA) in a tank-transfer apparatus (Bio-Rad Laboratories, Hercules, CA). The membranes were blocked with 5% skim milk in phosphate-buffered saline (PBS). Mouse anti-PEDF (TransGenic Inc., Hyogo, Japan) diluted 1:250 in blocking buffer was used as the primary antibody. Peroxidase-conjugated AffiniPure goat anti-mouse IgG (H + L) (Jackson ImmunoResearch Laboratories Inc., West Grove, PA) diluted 1:1,000 in blocking buffer was used as the secondary antibody. Enhanced chemiluminescence detection reagents (GE Healthcare, Buckinghamshire, UK) detected the antigens on the membrane. TotalLab TL120 software v2006 (Shimadzu Co.) quantified the intensity of each protein band; the intensity was used as an index of the level of protein expression.

Other Procedures

Serum levels of PEDF were determined by enzyme-linked immunosorbent assay (ELISAquant™ PEDF Sandwich ELISA Antigen Detection Kit [BioProducts MD, Middletown, MD]). Numerical data are presented as the mean ± standard deviation (SD). We evaluated the statistical significance using IBM SPSS Statistics 18 software (SPSS Inc., Chicago, IL). p Values less than 0.05 were considered significant.

RESULTS

Three-Step Proteome Analyses

Two serum samples from each of the 8 patients with alcohol abuse—one sample obtained on admission and the second, after 8 weeks of abstinence—were subjected to three-step serum proteome analysis. A representative CBB-stained SDS–PAGE gel (fraction No. 14) is shown in Fig. 1*A*. After converting the intensity of each band to a numerical value

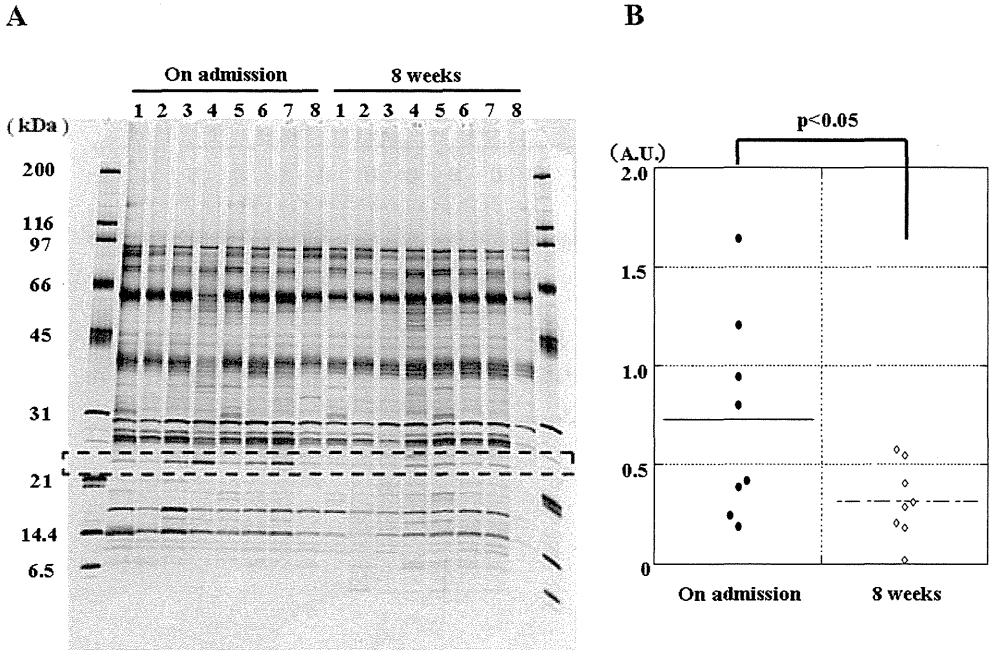

Fig. 1. Representative SDS–PAGE gel of an RP-HPLC fraction (fraction No. 14) and the comparison of the band intensities, as assessed by densitometry. Serum samples (100 μL each) were immunodepleted and injected onto the RP-HPLC column. Proteins in each fraction were subjected to 10 to 20% SDS–PAGE, as described in Methods. Following electrophoresis, the proteins were visualized using CBB staining. The image indicates the 25-kDa band that is equivalent to PEDF (**A**). The expression level of the 25 kDa band was quantified using densitometry in the 8 pairs of samples (i.e., 16 samples). The difference in the PEDF expression level is statistically significant (**B**). CBB, coomassie brilliant blue; ELISA, enzyme-linked immunosorbent assay; PEDF, pigment epithelial-derived factor; RP-HPLC, reverse-phase high-performance liquid chromatography; SDS–PAGE, sodium dodecyl sulfate polyacrylamide gel electrophoresis.